DEVELOPMENT OF ARGININE-CONTAINING WELL-DEFINED POLYMERS

A Thesis Submitted to
the Graduate School of Engineering and Sciences of
İzmir Institute of Technology
in Partial Fulfillment of the Requirements for the Degree of

MASTER OF SCIENCE

in Chemical Engineering

by
Damla TAYKOZ

July, 2014
İZMİR

We approve the thesis of **Damla TAYKOZ**

Examining Committee Members:

_____

Prof. Dr. Volga BULMUŞ
Department of Chemical Engineering, İzmir Institute of Technology

_____

Prof. Dr. Sacide ALSOY ALTINKAYA
Department of Chemical Engineering, İzmir Institute of Technology

_____

Prof. Dr. Mustafa DEMİR
Department of Materials Science and Engineering, İzmir Institute of Technology

8 July 2014

_____

Prof. Dr. Volga BULMUŞ
Supervisor, Department of Chemical Engineering
İzmir Institute of Technology

_____

Prof. Dr. Fehime ÖZKAN
Head of the Department of Chemical Engineering

_____

Prof. Dr. R. Tuğrul SENGER
Dean of the Graduate School of Engineering and Sciences

ACKNOWLEDGMENTS

I would love to thank Dr. Volga Bulmuş for her endless help. She has set an example of excellent researcher, mentor, and instructor to me**.** I have learned so much from her during this process. She supported me continuously and patiently. I also thank The Scientific and Technological Research Council of Turkey for funding my M.Sc. study through grant# 111T960. Plus, I am grateful to Salih Günnaz from Ege University, Fırat Ziyanak, Melih Kuş, Muhammed Üçüncü, Erman Karakuş, Doğan Taç for their help with NMR. Dr. Mustafa Demir for giving chance to perform my DLS experiments. Also, I would like to thank the staff of Biotechnology and Bioengineering Research and Application Center, especially Dane Rusçuklu. I am grateful to Dr. Gülistan Özçivici and Veysel Bay for providing me DNA samples. Also, I would love to thank to all people of Hacettepe University Chemical Engineering Department. I have learned so much from them.

I am grateful to my previous colleagues Tuğba Toker, Ekrem Özer and Işıl Kurtuluş. I cannot explain how much I am grateful to my labmates; Esra Aydınlıoğlu, İmran Özer, Vildan Güven and Aykut Zelçak. Their help and friendship let me to pass from dark side. I will always love them, our friendship is beyond lab borders. (Esra; TGIF! after 8:00 p.m. and saturday)

İpek Erdoğan, Mehmet Emin Uslu and Sedef Tamburacı are the best co-workers ever. If they and also Elif Karayel and Çiğdem Kahraman were not in my life, it was impossible to finish this work with having fun. Not only fun, it was literally impossible to finish.

Thanks to Sabrettin Umdu and Işın Dizvay for coming to my office and meeting me in their own way. We had much more fun than that should be in 2 years. Plus, Z-18 was the best office in IYTE at that times. Sezen Duygu Alıcı, Derya Köse, Elif Suna Sop, Melis Olçum. Thanks to them.

Also, I cannot find words to thank Melis Olçum and İbrahim Uzan. This part is beyond sentences. Of course Ceren Süngüç and Mehmet Çağlıyangil cannot be forgotten. Ceren is my childhood friend that I did not have chance to meet during our childhood.

Finally, I thank all of my family for supporting me during all my education. Special thanks goes to my dear mother Armağan Taykoz; my dear father Fikret Taykoz; my only and dearest sister Merve Taykoz for letting me through these days. They are the most patient, honest and loving people in my life.

ABSTRACT

DEVELOPMENT OF ARGININE-CONTAINING WELL-DEFINED POLYMERS

The aim of this work is to synthesize arginine-containing well-defined polymers via reversible addition-fragmentation chain transfer (RAFT) polymerization and perform preliminary investigation on the use of these polymers in nucleic acid complexation for potential gene therapy applications.

Pentafluorophenyl methacrylate (PFMA) was chosen as an active ester monomer to produce polymers having functional groups available for further modification. RAFT polymerization of PFMA was performed varying polymerization conditions such as feed composition and polymerization temperature. Polymers (PPFMA) were characterized using nuclear magnetic resonance (NMR) spectroscopy and gel permeation chromatography. Linear increase in $\ln[M]_0/[M]$ with polymerization time, and number average molecular weight (Mn) with monomer conversion indicated RAFT controlled polymerization of PFMA under the conditions tested. Furthermore, block copolymers of PFMA with poly(ethylene glycol) methacrylate (PEGMA) as a biocompatible component were prepared. Copolymerization was studied using both P(PFMA) and P(PEGMA) as macro RAFT agent. Copolymerization kinetic studies indicated that chain extension block copolymerizations were successfully performed using both macroRAFT agents. P(PFMA) was reacted with arginine methylester (AME) in the presence of triethylamine (TEA). 100% of P(PFMA) active ester groups could be modified with AME at a polymer/AME/TEA mole ratio of 1/1/3, as determined by ^{1}H-NMR spectroscopy. The AME modified polymers were complexed with a 681-bp DNA fragment through electrostatic interactions at varying nitrogen/phosphate (N/P) ratios. Gel electrophoresis experiments revealed that AME-modified P(PFMA) was able to complex with DNA at a N/P ratio of 200. Furthermore, the hydrodynamic diameter (D_h) of polymer/DNA complexes in phosphate buffer saline was found to be 58 nm, while the free DNA displayed a D_h of 109 nm, indicating the complexation of DNA by AME-modified P(PFMA).

ÖZET

ARJİNİN İÇEREN İYİ TANIMLANMIŞ POLİMERLERİN GELİŞTİRİLMESİ

Bu tezin amacı, iyi tanımlanmış arjinin içeren polimerlerin tersinir katılma ayrışma zincir transfer (RAFT) polimerizayonu ile sentezlenmesi ve potansiyel gen terapi uygulamaları için, arjinin içeren bu polimerlerin nükleik asit yapıları ile kompleks oluşturma kapasitelerinin incelenmesidir.

Polimerlerin üretilmesi için polimerizasyon sonrası modifikasyona uygun işlevsel gruplara sahip olan pentaflorofenil metakrilat (PFMA) polimerlerin üretilmesi için aktif ester monomer olarak seçildi. PFMA'nın RAFT polimerizasyonu besleme kompozisyonu ve sıcaklık gibi polimerizasyon koşullarını değiştirerek gerçekleştirildi. Polimerler (PPFMA) nükleer manyetik rezonans (NMR) spektroskopi ve jel geçirgenlik kromatografisi (GPC) kullanılarak karakterize edildi. $\ln[M]_0/[M]$ ve polimerizasyon zamanı ve moleküler ağırlık (Mn) ve dönüşüm arasındaki lineer ilişki, PFMA'nın denenen koşullarda RAFT kontrollü polimerizasyonunun gerçekleştiğini ortaya koydu. Buna ilaveten, biyolojik olarak uyumlu bileşen olan poli(etilenglikol) metakrilat (PEGMA) ile birlikte PFMA blok kopolimerleri hazırlandı. Kopolimerleşme reaksiyonlarında, makro RAFT ajanı olarak hem P(PFMA) hem de P(PEGMA) kullanıldı. Kopolimerleşme reaksiyonu kinetik çalışmaları göstermiştir ki; her iki zincir transfer ajanı kullanılarak yapılan kopolimerizasyonlar başarıyla sonuçlanmıştır. P (PFMA), trietilamin (TEA) varlığında arjinin metil ester (AME) ile reaksiyona sokulmuştur. P(PFMA)'nın aktif ester grupları %100 dönüşümle AME ile modifiye edilmiş ve sonuçlar ^{1}H-NMR spektroskopisi ile gösterilmiştir. AME ile modifiye polimerler değişen azot / fosfat (N/P) oranlarında, elektrostatik etkileşim yoluyla 681-bp DNA fragmanı ile karıştırılmıştır. Jel elektroforez deneyleri sonucunda AME-modifiye edilmiş P(PFMA)'nın, N/P:200 oranında DNA ile kompleks oluşturdukları görülmüştür. Ek olarak, fosfat tampon saline çözeltisi içerisinde ki polimer/DNA komplekslerinin hidrodinamik çapları (D_h) 58 nm olarak bulunmuştur. Serbest DNA'nın 109 nm hidrodinamik çapa sahip olması DNA'nın AME ile modifiye edilmiş P(PFMA) ile kompleks oluşturduğunu göstermektedir.

To my grandfather Hüsamettin Taykoz

TABLE OF CONTENTS

LIST OF FIGURES

Figure **Page**

LIST OF TABLES

Table **Page**

CHAPTER 1

INTRODUCTION

Nucleic acids such as DNA and RNA are used in pharmaceutical industries as potential therapeutics. It is known that these molecules have tremendous potential in treatment of various diseases including cancer and diabetes. However, effectively formulating and delivering them to the target cells are widely known challenges (Murthy, Campbell et al. 2003). Passing through the cellular membrane is one of the major problems to overcome. These potential therapeutics are originally cell membrane impermeable and they meant to reach cytosol to show their therapeutic effects (Carrasco 1994). Consequently, there is an urgent need for delivery systems that can help these molecules to cross cellular membranes and reach cytosol.

Polymers are one of the most important classes of materials used in drug delivery systems. They have played an integral role in the advancement of drug delivery technology by providing controlled release of therapeutic agents in constant doses over long periods, cyclic dosage, and tunable release of both hydrophilic and hydrophobic drugs. From early beginnings using off-the-shelf materials, the field of polymeric drug delivery systems has grown tremendously, driven in part by the innovations of chemical engineers. Modern advances in drug delivery are now predicated upon the rational design of polymers tailored for specific cargo and engineered to exert distinct biological functions including ability to insert therapeutic cargo through cellular membranes into cell cytosol (Liechty, Kryscio et al. 2010).

Cell-penetrating peptides (CPPs) have also attracted increasing attention for intracellular drug delivery applications. CPPs have provided an efficient intracellular delivery strategy for therapeutics that need to enter cell cytosol for biological activity, such as nucleic acid-based therapeutics. According to relevant literature, arginine richness improves the translocation efficiency of CPPs into cell.

The aim of this thesis is to synthesize well-defined arginine-containing polymers and perform preliminary investigation on the potential use of these polymers as nucleic acid carriers for intracellular drug delivery applications. Pentafluorophenyl methacrylate (PFMA) was chosen as an active ester monomer to produce polymers having functional

groups available for efficient modification with arginine. Reversible addition-fragmentation chain transfer (RAFT) polymerization was used to produce well-defined polymers as it is one of the most amenable techniques to the synthesis of polymers for biomedical applications. The procedures for polymer synthesis, modifications and characterizations are presented in Chapters 3. Chapter 4 covers the results of synthesis of PFMA monomer, RAFT polymerization kinetics studies, copolymerization studies of PFMA with PEGMA, arginine reaction of PFMA polymer and DNA complexation of arginine modified polymer.

CHAPTER 2

LITERATURE REVIEW

2.1. Intracellular Drug Delivery

Over the past three decades, significant developments have been made in drug delivery systems. It has become an interdisciplinary research topic covering engineering, biotechnology and medicine.

An ideal drug delivery system aims to improve bioavailability, therapeutic index, patient acceptance or compliance (Vasant V. Ranade, 2011).

Biological molecules such as DNA, RNA and proteins have an important role and wide variety in the biotechnology and pharmaceutical industries. In the last three decades, they have been developed as potential therapeutics. It is known that these molecules have tremendous potential in treatment of various diseases. However, effectively formulating and delivering them to the target are widely known challenges.

These challenges are due to the fact that therapeutic DNA, RNA and protein molecules have *low biomembrane permeability* (Lindgren, Hällbrink et al. 2000), *low bioavailability, systemic toxicity, in vivo instability, high hepatic and renal clearance rates, and high cost of manufacturing*. Drug delivery systems overcome these challenges of the biological molecules when they directly administrated (Han, Mahato et al. 2000).

Viruses and toxins are thought to be the solution of these problems. Because they can carry multi-functional biomolecules which can be recognized by the cell membrane easily and have enhanced transport mechanism to the cytosol (Murthy et al., 2003).

Viruses can carry their genetic information through the following steps: Firstly, they pack the viral genome (Smith and Helenius 2004), then circulate through the blood stream and bind to cell surface receptors. They pass the internalization pathways into cells. Secondly, they escape from endocytic vesicles and finally deliver their genome to the nucleus. Simple viruses cross cell plasma membrane easily. However, complex viruses enter the cell via endocytosis (Mudhakir and Harashima 2009).

2.2. Cell-Penetrating Peptides

Cell-penetrating peptides (CPPs) have attracted increasing attention for intracellular drug delivery. CPPs have provided a non-invasive, biocompatible, and efficient intracellular delivery strategy for therapeutics that need to enter cell cytosol for biological activity, such as nucleic acid-based therapeutics (Fonseca, Pereira et al. 2009). CPPs are peptides that are able to interact with cell-membrane (Zorko and Langel 2005) and enhance cellular uptake of various molecules.

Peptide length, chemical properties and size are important parameters for cell uptake of CPPs. Increasing the peptide length (changing the number of repeating units) increases the activity of CPPs. However increasing the size of CPPs may not increase the activity (Piantavigna, McCubbin et al. 2011). Also, it has been studied that presence of positive charge (especially arginine residues) are very important in the uptake mechanism (Madani, Lindberg et al. 2011). Furthermore, uptake mechanism is also substantial. It has been shown that CPPs cell uptake utilized two routes: energy-dependent mechanism (endocytosis) or translocation of the lipid bilayer (see Figure 2.1) (Stewart, Horton et al. 2008).

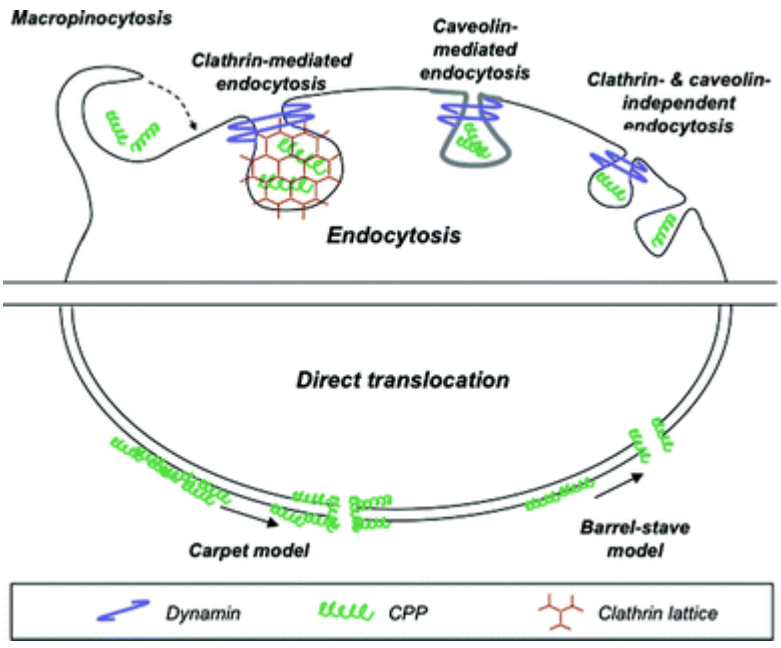

Figure 2.1. Examples of CPPs uptake mechanisms
(Source: Stewart et al., 2008)

CPPs are peptide sequences with the ability to cross cellular membranes (Katayama, Hirose et al. 2011). Hence, they have been used to enhance the uptake of molecules into cells. For example, incorporation of a CPP with a fluorescently labelled protein promoted *in vitro* uptake of acid-degradable polyacrylamide particles (microparticles) in non-phagocytic epithelial cells (Cohen, Almutairi et al. 2008).

According to the study by Cohen et al. (see Figure 2.2) CPP modification increases the uptake of microparticles by BEAS-2 cells, a non-phagocytic cell line. As it can be seen in Figure 2.2/A CPP modified microparticle uptake was found to be greater than the uptake of the particles without CPP modification. Figure 2.2/B shows the time dependency of the cell uptake. After 2 hours, most of the microparticles appear on the cell surfaces. Within 24 hours, intracellular accumulation has increased. Figure 2.2/C shows that when concentration of CPP was increased, the florescence in the cells hence the uptake of acid-degradable polyacrylamide particles increased.

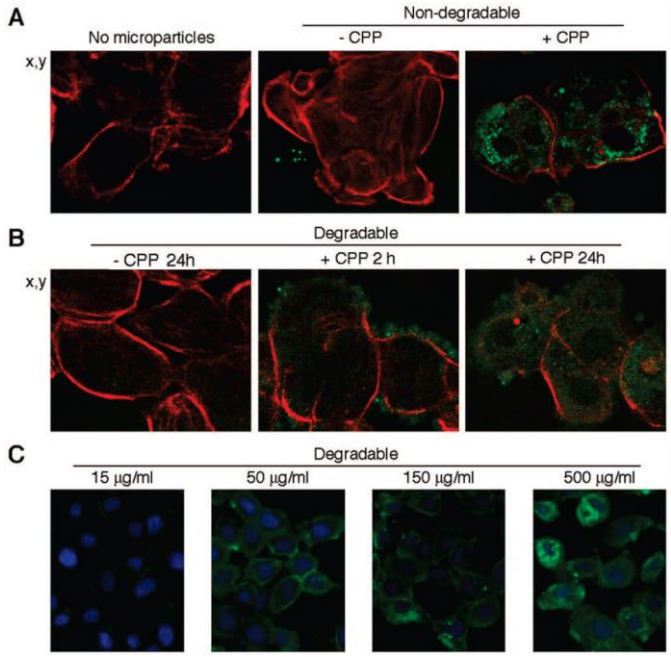

Figure 2.2. A: The cellular accumulation of CPP-modified microparticles 500 μg/ mL, B: Time dependency, C: Concentration dependency (Source: Cohen et al., 2008)

Examples for commonly used CPPs are shown in Table 2.1. In this table, some of the examples are extracted from natural sequences (Tat and penetratin), and other CPPs are artificially designed and synthesized in the scope of important features of natural systems (Stewart et al., 2008).

Table 2.1. Examples of CPP sequences

Cell-penetrating peptide	Amino acid sequence
Polyarginines	**RRRRRRRRR** (R_9)
$Tat_{49–57}$	**RKKRR**Q**RRR**
Penetratin (Antennapedia)	**R**QI**K**IWFQN**RR**M**K**W**KK**
Pep-1	**K**ETWWETWWTEWSQP**KKKRK**V
Transportan	GWTLNSAGYLLG**K**INL**K**ALAALA**KK**IL
Nuclear localization sequences	VQ**RKRQK**LMP
	S**KKKKIK**V
	G**RKRKKR**T

For example the human immunodeficiency virus (HIV)-1 Tat protein has an arginine-rich peptide segment. It is known that this virus penetrates and translocates into cell very easily and efficiently. It has been shown that mimicking these structures can overcome the intracellular delivery problem of complex biomacromolecular therapeutics. It is known that arginine-rich oligopeptides show very similar properties as a delivery vector (Futaki 2005).

2.3. Arginine Rich CPPs

CPPs that contain arginine segments constitute efficient components of intracellular drug delivery systems (Futaki, 2005).

According to relevant literature, arginine richness improves the translocation efficiency of the molecule into cell (Table 2.2) (Futaki, 2005). Advantages of arginine arise from arginine amino acid binds to phosphate groups of phospholipid bilayer and

causes a strong distortion and water pore formation. Translocation of arginine then occurs due to this distortion (Herce et al., 2009).

Table 2.2. Tat analogs translocation efficiency
(Source: Futaki, 2005)

Peptides	**Sequences**	**Translocation Efficiency**
Tat and the related peptides		
HIV-1 Tat(48-60)	GRKKRRQRRRPPQ	+++
D-Tat	*GRKKRRQRRRPPQ*	+++
R_9-Tat	GRRRRRRRRRPPQ	+++
Arginine-rich RNA binding peptides		
HIV-1 Rev-(34-50)	TRQARRNRRRRWRERQR	+++
FHV Coat-(35-49)	RRRRNRTRRNRRRVR	+++
BMV Gag-(7-25)	KMTRAQRRAAARRNRWTAR	+++
HTLV-II Rex-(4-16)	TRRQRTRRARRNR	+++
CCMV Gag-(7-25)	KLTRAQRRAAARKNKRNTR	++
P22 N-(14-30)	NAKTRRHERRRKLAIER	++
λ N-(1-22)	MDAQTRRRERRAEKQAQWKAAN	+
φ 21 N-(12-29)	TAKTRYKARRAELIAERR	+
Yeast PRP6-(129-144)	TRRNKRNRIQEQLNRK	+
Human U2AF-(142-153)	SQMTRQARRLYV	-

The number of repeating arginine units and arginine conformation were found to be important in translocation efficiency of arginine-rich peptides. Figure 2.3 shows the results of the *in vivo* study of oligoarginine peptides having different arginine content and conformation. Peptides were labelled with Alexa660 fluorescent dye and the *in vivo* accumulation in mice was investigated. According to this study, D-arginine with 8 arginine units has the highest uptake. However, D-arginine is known to be toxic to the body. Considering this fact, L-arginine with 8 units (R8) was found to have the most efficient uptake into body.

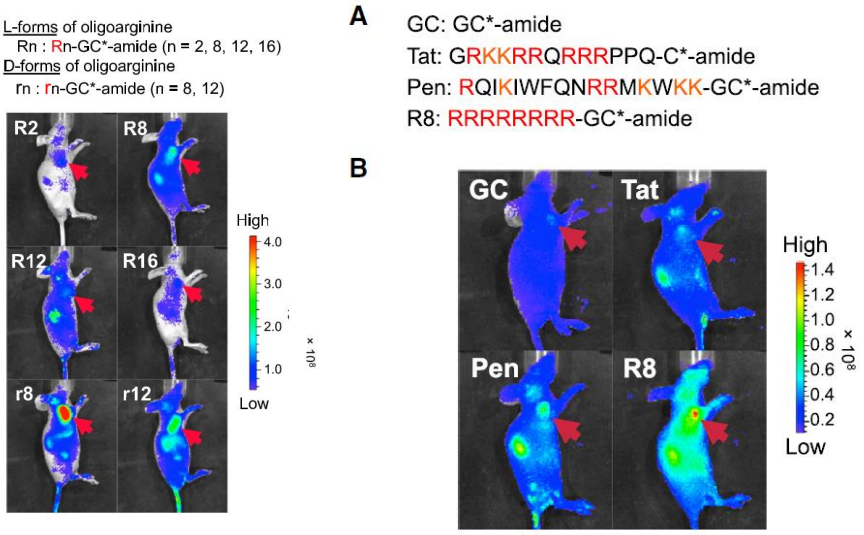

Figure 2.3. Tumor accumulation of fluorescently labeled oligoarginine peptides intravenously administrated into tumor-bearing mice. (A) Structures of oligoarginine peptides bearing the GC-amide segment at the C-termini for the labeling with Alexa660. R and r represent L- and D-arginines, respectively. C* denotes Alexa660-labeled L-cysteine. (B) *In vivo* fluorescent imaging of tumor-xenografted mice at 24 h after intravenous injection of Alexa660-labeled oligoarginine peptides and CPPs (3 nmol each). Red arrows represent tumor xenografts (Source: Nakase, Konishi, Ueda, Saji, & Futaki, 2012)

Additionally, comparison of R8 peptide, TAT protein and Pen (derived from amino acids 43–58 of the Antennapedia homeo-protein) has shown that after 24 hours R8 was taken in highest compared to TAT and Pen (see in Figure 2.3). TAT and Pen were chosen for their well-known membrane permeability.

Combining R8 with a hydrophobic segment may increase the interaction of the molecule with the cell membrane. Thus, molecules with different carbon content were combined with R8 and their cell internalization was investigated. According to Figure 2.4 combining hexanoic acid with R8 (C6R8) showed the best cell internalization when compared with itself and butanoic acid with R8 (C4R8). These results suggest that combining arginine-rich peptides with hydrophobic structures having increasing number of alkyl units increases the uptake of the molecule. This can be explained by the increased amphiphilicity of the final molecule and increasing the cell membrane perturbation. Furthermore, experiments at 4^{o}C showed better internalization, indicating direct membrane translocation which is an energy-independent uptake mechanism.

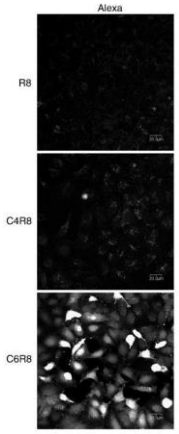

Figure 2.4. The HeLa cells were incubated with acylated R8 peptides labeled with Alexa488 (10 μM) for 30 min at 37 °C (Source: Katayama et al., 2011)

Another study showed arginine content in a CPP improves the cellular uptake. According to Figure 2.5 HR9/QD (Hystidine-R9-Quantum Dot) complex passes through cell membrane. It was also found that the complex interacts with the cell membrane within a short time period (4 min). Interestingly, internalization of the complex at 4^{o}C by cell membrane was also observed, which shows that systems containing arginine-rich peptides use an energy-independent pathway for crossing cellular membranes.

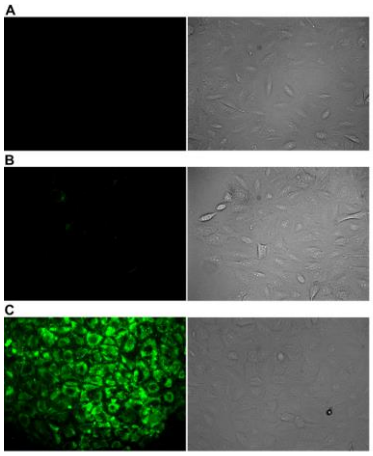

Figure 2.5. Confocal microscopy of intracellular delivery of CPP/QD complexes into A549 cells. A: Internal control. Human A549 cells without any treatments were observed under the GFP channel (left column) or transmitted light (right column) at a magnification of 200 x. B: Negative control. Cells treated with QDs only for 1 h. C: Treatment with HR9/QD (60:1) complexes for 1 h (Source: Liu, Huang, Winiarz, Chiang, & Lee, 2011)

2.4. Arginine Containing Polymers

Relevant literature implies that arginine content in a drug delivery system improves the intracellular delivery efficiency of the system. It can be easily envisioned that combining arginine with a polymeric structure potentially provides a variety of enhanced properties such as stability, amphiphilicity stimuli-responsive and electrostatic properties, which improves biological function of the system.

Kim et al. investigated PAMAM-PEG-PAMAM (PPP) dendritic copolymer and its combination with arginine (PPP-R) (Figure 2.6).

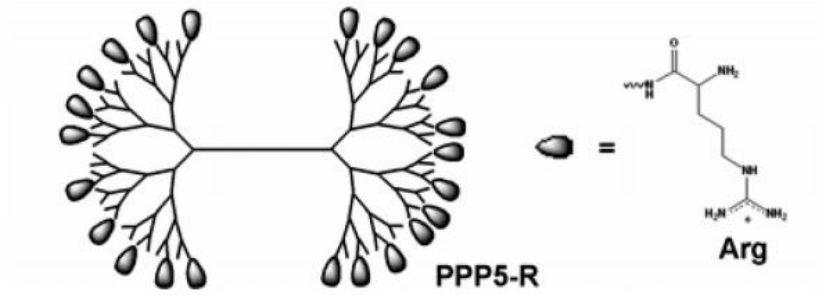

Figure 2.6. Structure of arginine modified dendritic copolymer of PAMAM-PEG (Source: Kim et al., 2007)

The transfection efficiency of the arginine grafted dendritic copolymer was 20-36 times higher than that of the unmodified dendritic copolymer, PPP5 (Figure 2.7).

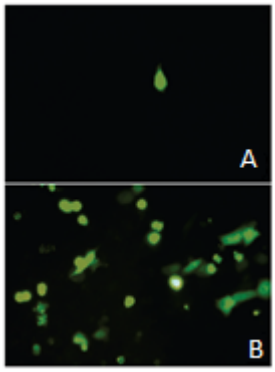

Figure 2.7. GFP expression in HeLa cells by PPP5 (A) and PPP5-R (B), respectively (Source: Kim et al., 2007)

Amine terminated PEG-coated iron oxide nanoparticles (NPs) with a 12-nm core diameter were synthesized and combined with polylysine (pLys), poly-arginine (pArg) or polyethylenimine (PEI) for complexation of small interfering RNA (siRNA) (Figure 2.8). While NP-pLys-siRNA and NP-PEI-siRNA complexes were observed to enter the cell through endocytic pathway, NP-pArg-siRNA appeared to translocate directly through cell membrane (Figure 2.9a). Furthermore, NP-pLys-siRNA and NP-PEI-siRNA complexes were found to escape from endosomal vesicles while NP-pArg-siRNA complex was found to exist in the cytosol with no visible endosomal vesicle (Figure 2.9b).

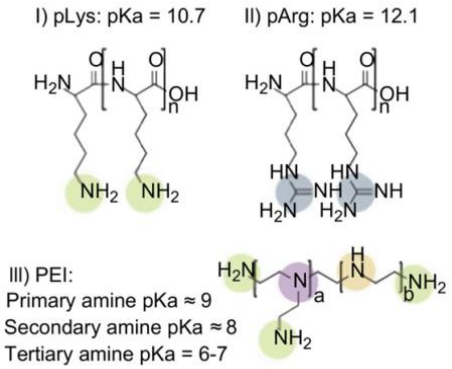

Figure 2.8. Structures of pLys (I), pArg (II) and PEI (III) (Source; Veiseh et al., 2011)

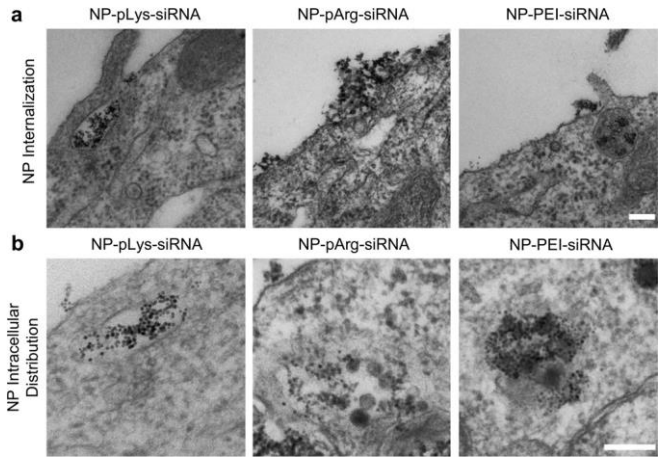

Figure 2.9. TEM images of C6/GFP$^+$ cells treated with three different nanovector formulations. a) Internalization of nanovectors. b) Intracellular localization of nanovectors. Scale bars represent 250 nm (Source: Veiseh et al., 2011)

In another study mesenchymal stem cells (MSCs) were studied using upconversion nanoparticles (UCNPs) coated with arginine-modified polyethylene glycol (PEG). As it can be seen in Figure 2.10 arginine modified system shows better luminescence (UCL) emission than unmodified system, indicating a better uptake profile of arginine-modified system.

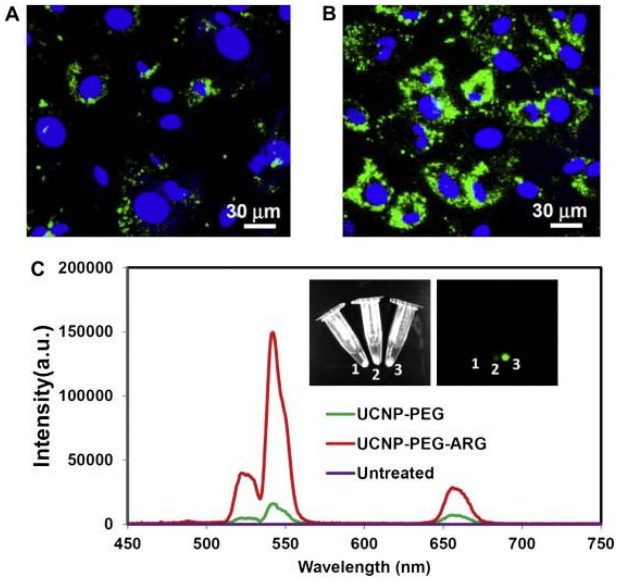

Figure 2.10. Comparison of cell transfection efficiency of UCNP-PEG and UCNP-PEG-ARG. (A&B) Laser scanning confocal microscopy images of mMSCs incubated with UCNP-PEG (A) or UCNP-PEG-ARG (B) for 4 h. (C) UCL spectra of trypsinizedmMSCs incubated with UCNP-PEG or UCNP-PEG-ARG recorded by a modified Maestro in vivo imaging system. Inset: a bright field photo and a UCL image of untreated (left, 1), UCNP-PEG treated (middle, 2) and UCNP-PEG-ARG treated (right, 3) mMSCs in test tubes (Source: Wang, Cheng, Xu, & Liu, 2012)

Guanidine group containing polymers (GPMA) which are very similar to arginine containing polymers, and their copolymers with hydroxypropylmethacrylamide (HPMA) have been synthesized as shown in Figure 2.11, and tested for their cell entering abilities. Copolymers of GPMA and HPMA were found to enter cells much more efficiently when compared to PGPMA itself and PHPMA.

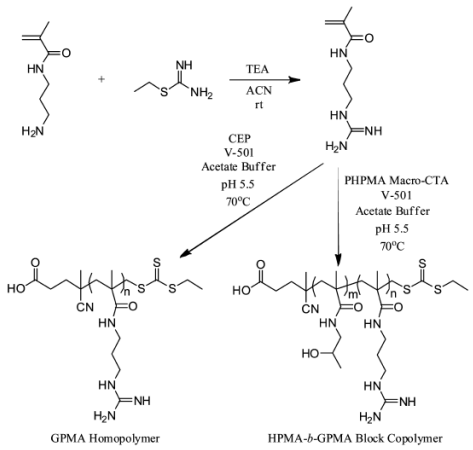

Figure 2.11. Synthesis of 3-Guanidinopropyl methacrylamide (GPMA) and subsequent *a*RAFT polymerization of the monomer to form a GPMA homopolymer and HPMA block copolymer (Source: Treat et al., 2011)

2.5. Active Ester Polymers

Active ester presence provides easy reactivity for peptides in organic chemistry. The use of polymeric activated esters was originated in the 1970s, (Ferruti, Bettelli, & Feré, 1972) and (Batz, Franzmann, & Ringsdorf, 1972) polymerized N-(meth)acryloxysuccinimides for the first time via free radical polymerization (Beija, Li, Lowe, Davis, & Boyer, 2013). These active ester polymers, i.e. prepolymers, enable the preparation of complex and functional polymers through their reactive functional pendant groups (Eberhardt, Mruk, Zentel, & Théato, 2005).

Active ester monomers are highly reactive and specific with primary or secondary amine-containing molecules through the formation of amide bonds. These reactive polymers can be easily used to generate functional homo or random copolymers by post-polymerization modification reactions (see Figure 2.12) (Eberhardt et al., 2005).

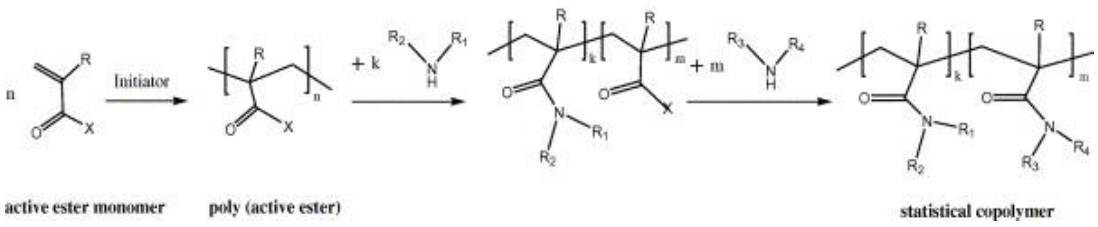

Figure 2.12. Synthesis of active ester polymers and their reaction with amines (Source: Eberhardt et al., 2005)

It is known that there are a number of activated ester monomers (Theato, 2008). Among these, pentafluorophenyl esters proved to be very effective in peptide chemistry (Eberhardt et al., 2005). A very powerful activated ester includes the derivatives of pentafluorophenyl acrylates. They have relatively high-hydrolytic stability, improved solubility in organic solvents and can be prepared via enhanced polymerization techniques such as Reversible Addition Fragmentation Chain Transfer Polymerization (RAFT) (Gibson, Fröhlich, & Klok, 2009).

It is important to state that even the importance of pentafluorophenyl activated ester chemistry grows, copolymerization of pentafluorophenyl ester monomers with a hydrophilic monomer has not yet received much attention (Beija et al., 2013).

2.6. Modification of Pentafluorophenyl methacrylate (PFMA) with Arginine

It was shown that poly(pentafluorophenyl methacrylate) (PPFMA) are highly reactive towards various amines including arginine amino acid (Figure 2.13). It is important to note that the reaction between arginine amino acid and active ester polymer is highly selective and occurs between alpha-amino group of the amino acid and the active ester group of the polymer. In other words, it does not involve the functional guanidine group of arginine molecules.

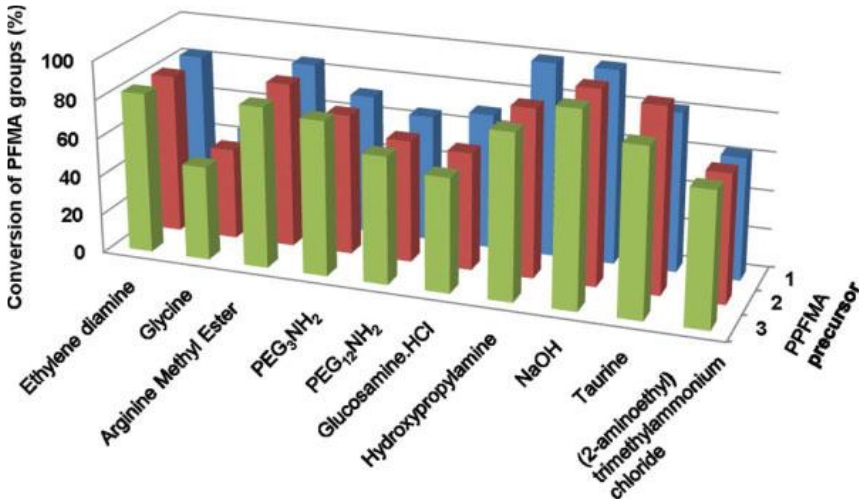

Figure 2.13. Degree of conversion of PPFMA precursors of different molecular weight after postpolymerization modification with a range of different functionalized amines (Source: Gibson et al., 2009)

In a study by Nuhn et al., copolymers of PFMA and triethyleneglycolmethyl ether methacrylate (MEO_3MA) were synthesized and modified with arginine for complexation with siRNA. It was shown that copolymers of MEO_3MA and PFMA after modification with arginine were able to form nanoplexes with siRNA and these nanoplexes were internalized by cells in a time-dependent manner (Figure 2.14).

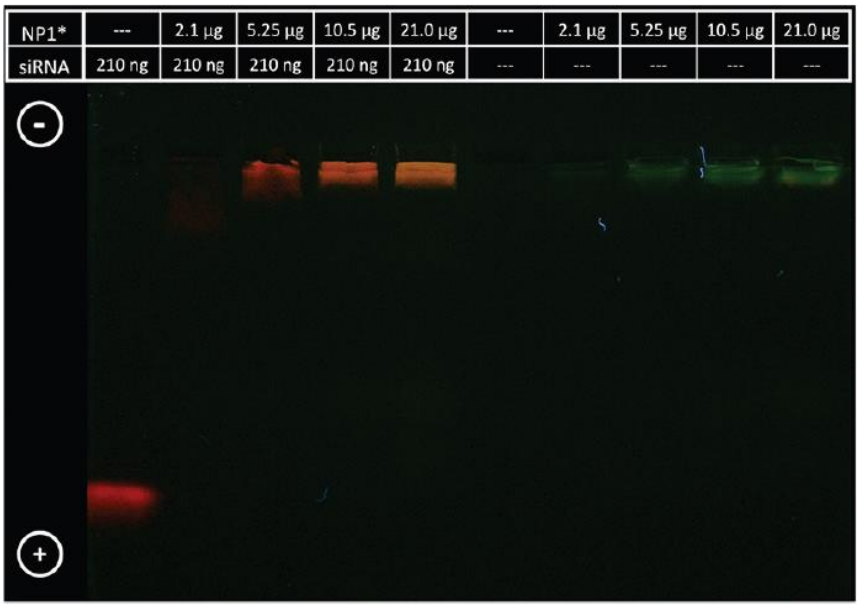

Figure 2.14. Agarose gel (0.5%) electrophoresis at 90 V for 50 min of various weight to weight ratios of NP1* (green) to siRNA (red) as indicated in the panel in the upper part of the image. The orientation of the electric field is indicated by symbols of the plus and minus poles (Source: Nuhn et al., 2012)

2.7. Reversible Addition-Fragmentation Chain Transfer (RAFT) Polymerization

While preparing a polymeric drug delivery system, it is very important to have the control over certain characteristics of the macromolecules. These characteristics can be listed as architecture, molecular weight, composition, and polydispersity index. In an ideal polymeric drug delivery vehicle, all these characteristics need to be well-defined. Reversible Addition-Fragmentation Chain Transfer (RAFT) Polymerization enables the synthesis of polymers with all these properties well-defined. Advantages of the RAFT polymerization are listed below: (Boyer, Bulmus et al. 2009)

1. Using the RAFT technique it is possible to synthesize polymers having various architectures including linear polymers, block and graft copolymers, brush or comb-type and star polymers (Gregory & Stenzel, 2012).

2. RAFT technique enables the synthesis of polymers with controlled molecular weights and low polydispersity (PDI).

3. RAFT polymerization is compatible with a wide variety of monomers, solvents, functional groups, and polymerization conditions.

RAFT process was firstly reported by CSIRO group in 1998. Since then it has become one of the important techniques for the synthesis of polymers for drug and gene delivery vehicles. Synthesis of amphiphilic, water-soluble structures via RAFT polymerization with all its advantages is easy to achieve (York, Kirkland et al. 2008).

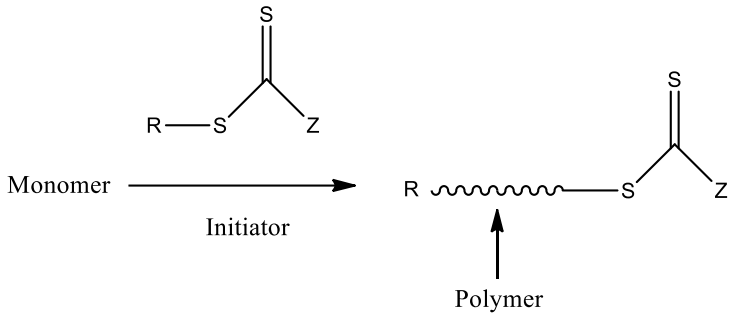

Figure 2.15. Simple illustration of RAFT mechanism

The presence of a special chain transfer agent, the RAFT agent differs this special polymerization technique from conventional radical polymerization techniques. Polymerization steps and mechanisms are nearly same for both polymerizations. The main difference is as in Figure 2.15 thiocarbonylthio group (S-C=S) of the RAFT agent (Stenzel, 2008).

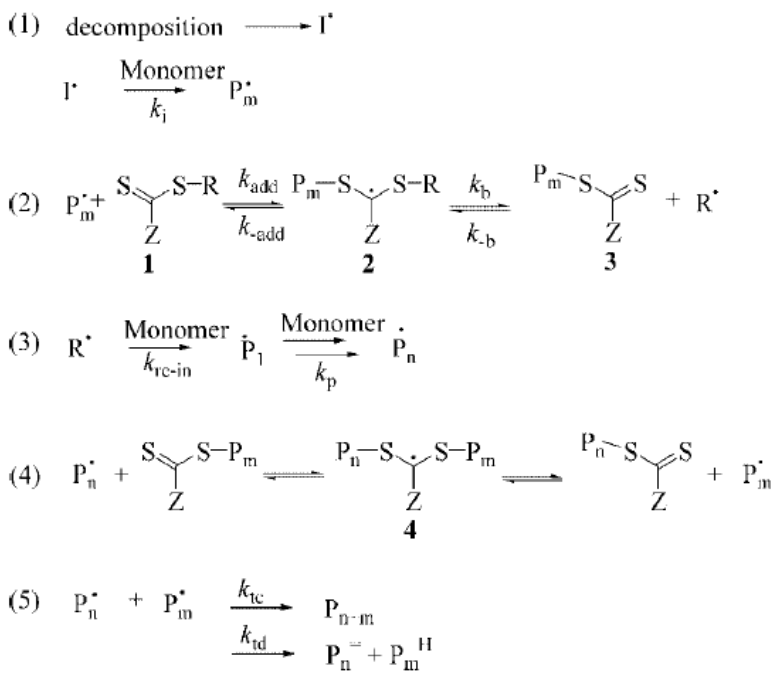

Figure 2.16. Detailed mechanism of RAFT polymerization
(Source: Boyer et al., 2009)

In the first step of polymerization, initiator is decomposed and oligomeric radicals are produced (step 1). Then, due to highly reactive C=S bond, as explained before, this oligomeric radicals interact with RAFT agent and produces radical intermediate (2), original RAFT agent (1) and oligomeric RAFT agent and initiator radical (3). Step 2 is always in an equilibrium and these structures convert to each other. RAFT agent's R group is very important to have quick fragmentation property. This step is the rate controlling step for the RAFT technique. Thus, the produced radical (3) interacts with other monomers and other oligomeric radicals are produced (step 3). Oligomeric radical activates oligomeric RAFT molecules and when C=S bond is shifted, then RAFT agent conjugated to the oligomeric radical it becomes an oligomeric RAFT molecule and initial oligomeric RAFT molecule becomes an oligomeric radical (step 4). Reaction conditions are very important to control these interactions between oligomeric structures. Termination occurs with both combination and disproportionation mechanism (step 5) (Boyer et al., 2009).

CHAPTER 3

MATERIALS AND METHODS

3.1. Materials

For the synthesis of pentafluorophenyl methacrylate (PFMA) (Eberhardt, Mruk et al. 2005) pentafluorophenol (ReagentPlus® 99% purity), 2-6 lutidine (ReagentPlus® 98% purity) and methacryloyl chloride (97% purity) were purchased from Sigma-Aldrich. Dichloromethane (for organic trace analysis UniSolv®) was purchased from Merck. Aluminum oxide (Geduran® Al 90) for column chromatography was obtained from Merck. For RAFT polymerization of PFMA (Eberhardt, Mruk et al. 2005); chain transfer agent, 4-cyano-4-(phenylcarbonothioylthio) pentanoic acid (CPADB) was purchased from Sigma-Aldrich. 2,2′-Azobis(2-methylpropionitrile) (AIBN) was used as an initiator after recrystallization twice in methanol. 1,4-Dioxane (ACS Reagent 99% purity) was purchased from Sigma-Aldrich. Hexane (anhydrous 95% purity) was bought from Sigma-Aldrich. L-Arginine methyl ester dihydrochloride (98% purity) and L-Arginine were purchased from Sigma-Aldrich (Gibson, Fröhlich et al. 2009). Poly(ethylene glycol) methyl ether methacrylate (PEGMA; Mw:467 g/mol), N,N-dimethylacetamide (DMAc) (CHROMASOLV® Plus, for HPLC, ≥99.9% purity), lithium bromide, diethylether, triethylamine (TEA), deuterium oxide (D_2O), deuterium chloroform ($CDCl_3$), deuterated dimethyl sulfoxide (DMSO-d_6), N,N-dimethylformamide (DMF) were purchased from Sigma-Aldrich.

Dialysis membrane (MWCO = 1000-10000 Da) was purchased from Spectrum® Laboratories. Citric acid and mono, dibasic phosphate salts and magnesium sulfate were purchased from Merck.

3.2. Instruments

3.2.1. Gel Permeation Chromatography

Molecular weight and molecular weight distribution (polydispersity index) of polymers were determined by gel permeation chromatography. A Shimadzu modular system comprising an SIL-10AD auto injector, PSS Gram 30 Å and 100 Å (10 μM, 8x300 mm) columns, an RID-10A refractive-index detector and SPD- 20A prominence UV/vis detector calibrated with low polydispersity poly(methyl methacrylate) standards (410-67000g/mol) were used. The mobile phase was N, N dimethylacetamide (DMAc) containing 0.05 % w/v LiBr.

3.2.2. Nuclear Magnetic Resonance Spectroscopy

^{19}F-NMR and ^{1}H-NMR spectroscopy (Varian, VNMRJ 400 spectrometer) was used to determine the chemical structure of synthesized compounds and both the reaction yields and polymerization conversions. Deuterium oxide (D_2O), chloroform ($CDCl_3$) and deuterated dimethyl sulfoxide (d_6) were used as NMR solvents. For NMR analysis, samples were dissolved at approximately 10 mg/ml concentration.

3.2.3. UV-Visible Spectrophotometry and DLS Analysis

UV-visible light absorbance of the solutions was measured by a Thermo Scientific Evolution 201 UV-visible spectrophotometer using quartz cuvettes.

For DLS analysis, Malvern NanoZS Particle Analyzer was used to determine hydrodynamic diameter of polymers and their DNA complexes.

3.2.4. Agarose Gel Electrophoresis

Gel electrophoresis experiment was done with using a Thermo Scientific Owl™ EasyCast™ B1 mini gel system. 1% agarose gel stained with ethidium bromide was used in this system.

3.3. Methods

3.3.1. Synthesis of Pentafluorophenyl Methacrylate

Pentafluorophenyl methacrylate (PFMA) was synthesized according to literature (Eberhardt, Mruk, Zentel, & Théato, 2005). Reaction scheme is in Figure 3.1.

Pentafluorophenol (0.6 M; 5 g; 27.2 mmol) was dissolved in dry DCM (46.4 mL) in a round bottom flask and then 2.6-lutidine (3.255 mL; 27.9 mmol) was added. The solution was degassed by purging nitrogen. Finally, methacryloyl chloride (2.78 mL; 30.3 mmol) was added slowly and reaction mixture was stirred at 0^{o}C during 3 hours. The reaction medium was then kept at room temperature overnight. Extraction of the reaction mixture was performed with water, and DCM phase was collected and dried over magnesium sulfate. Vacuum distillation was then performed to obtain the product. The distillation was carried out at 50^{o}C-60^{o}C and 10 mbar. Finally, column chromatography was performed in order to remove methacrylic acid residues. The final product, PFMA was analyzed via ^{1}H-NMR and ^{19}F-NMR in $CDCl_3$.

^{1}H-NMR ($CDCl_3$): δ in ppm: 6.43 (1H, t, J_{HH} = 2 Hz), 5.89 (1H, t, J_{HH} = 1.5 Hz), 2.06 (3H, t, J_{HH} = 1.5 Hz);

^{19}F NMR (CDCl3): δ in ppm: -162.90 (2F, dd, J_{FF} = 12 and 18 Hz), -158.63 (1F, t, J_{FF} = 15 Hz), -153.17 (2F, d, J_{FF} = 15 Hz).

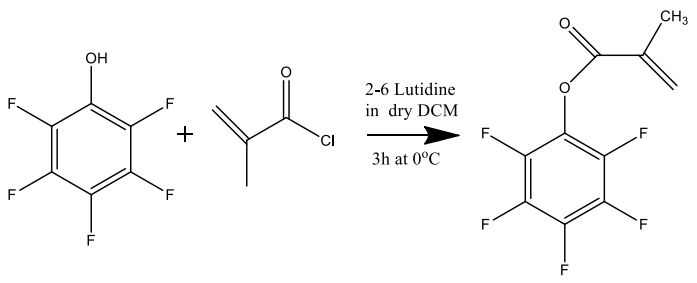

Figure 3.1. Synthesis of PFMA

3.3.2. RAFT Polymerization of Pentafluorophenyl Methacrylate (PFMA)

Polymerization scheme of PFMA is given in Figure 3.2. In polymerization of PFMA, initiator and the RAFT agent were azobisisobutyronitrile (AIBN) and 4-cyano-4 (phenylcarbonothioylthio) pentanoic acid, respectively.

Polymerization scheme of PFMA is given in Figure 3.2. In polymerization of PFMA, initiator and the RAFT agent were azobisisobutyronitrile (AIBN) and 4-cyano-4 (phenylcarbonothioylthio) pentanoic acid, respectively.

PFMA (2 M; 200 mg; 0.8 x 10^{-3} mol), RAFT Agent and AIBN were dissolved in dioxane. The ratios of reagents are given in Table 3.1. Before polymerization, the reaction mixture was purged with nitrogen for about 15 minutes in order to remove oxygen from the medium. The mixture was sealed and then put into an oil bath set at a given temperature as shown in Table 3.1, summarizing conditions used for all polymerizations. Polymerization was stopped by immersing the solution into an ice bath and exposing it to the air. After ^{1}H-NMR analysis of the reaction medium for determination of monomer conversion (Equation 3.1), reaction medium was purified by dissolving in DCM and precipitating into hexane. The purification procedure was repeated three times. The solid phase was then collected and samples were analyzed using ^{1}H-NMR and ^{19}F-NMR in $CDCl_3$. Furthermore, GPC analyses of poly(pentafluorophenyl methacrylate) (PPFMA) samples were performed to determine molecular weights and molecular weight distributions of the polymers. Number average molecular weights (M_ns) were also determined from ^{1}H-NMR spectra of purified polymers, as given in Equation 3.2 below.

^{1}H NMR ($CDCl_3$): δ in ppm: 2.41 (2H, br s), 1.38 (3H, br s);

^{19}F NMR ($CDCl_3$): δ in ppm: -161.33 (2F, br s), -156.2 (1F, br s), -151.77 (2F, br s)

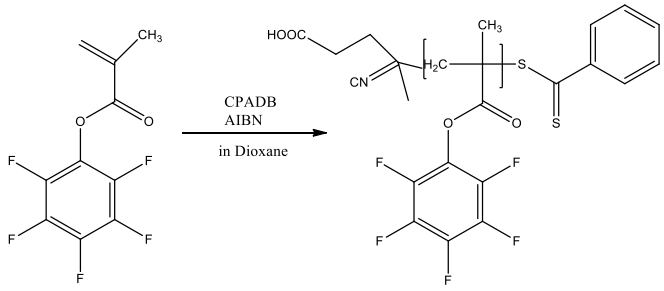

Figure 3.2. Polymerization scheme of PFMA

Table 3.1. Reaction conditions for PFMA polymerization

Sample Code	[M]/[R]/[I]	Time (min)	Sample Code	[M]/[R]/[I]	Time (min)
Dioxane at 90°C			Dioxane at 80°C		
DT-5/15min	50/1/0.25	15	DT-10 / 7Min	25/1/0.25	7
DT-5/30min	50/1/0.25	30	DT-10 / 15Min	25/1/0.25	15
DT-5/60min	50/1/0.25	60	DT-10 / 22Min	25/1/0.25	22
DT-5/120min	50/1/0.25	120	DT-10 / 30Min	25/1/0.25	30
Dioxane at 90°C			Dioxane at 80°C		
DT-7/7min	100/1/0.25	7	DT-9 / 7min	100/1/0.125	7
DT-7/15min	100/1/0.25	15	DT-9 / 15min	100/1/0.125	15
DT-7/22min	100/1/0.25	22	DT-9 / 22min	100/1/0.125	22
DT-7/30min	100/1/0.25	30	DT-9 / 30min	100/1/0.125	30
Dioxane at 90°C			Dioxane at 80°C		
DT-6/7min	25/1/0.25	7	DT-11 / 7Min	25/1/0.125	7
DT-6/15min	25/1/0.25	15	DT-11 / 15Min	25/1/0.125	15
DT-6/22min	25/1/0.25	22	DT-11 / 22Min	25/1/0.125	22
DT-6/30min	25/1/0.25	30	DT-11 / 30Min	25/1/0.125	30

$$\text{Conversion } \% = \frac{(\int_{2,41} \text{Polymer})/2}{(\int_{2,41} \text{Polymer})/2 + \int_{6,43} \text{Monomer}} \text{ x } 100 \qquad (3.1)$$

$$Mn\ NMR = \frac{\int Polymer}{\int RAFT}\ x\ Mw\ of\ Monomer + Mw\ of\ RAFT \qquad (3.2)$$

3.3.3. RAFT Polymerization of Poly(ethylene glycol) Methyl Ether Methacrylate (PEGMA)

Poly(ethylene glycol) methyl ether methacrylate (PEGMA (Mn: 467 g/mol) Repeating Unit: 7-8) was polymerized via RAFT polymerization using AIBN as an initiator and 4-cyano-4 (phenylcarbonothioylthio) pentanoic acid as a RAFT agent.

PEGMA (Mw: 475 g/mol, [1 M], 5 g, 10.5 mmol) and RAFT Agent (Mw: 279 g/mol, 0.0585 g, 0.21 mmol) and AIBN (Mw: 164 g/mol, 0.00861 g, 0.0525 mmol) were dissolved in ACN (10,5 mL). Before polymerization, the reaction mixture was purged with nitrogen for about 15 minutes in order to remove oxygen from the medium. The mixture was sealed and then put into an oil bath set at 65ºC for 100 min. Polymerization was stopped by immersing the solution into an ice bath and exposing it to the air. The reaction medium was purified by dissolving in water and dialyzed against a dialysis tubing with a MWCO 3500 for 5 days.

3.3.4. Copolymerization of PFMA and PEGMA

Block copolymers of PFMA and PEGMA were prepared via RAFT polymerizations using either PPFMA or poly(poly(ethylene glycol) methyl ether methacrylate) (PPEGMA) as a macroRAFT agent. In a typical copolymerization procedure where PPFMA was used as a macroRAFT agent, PPFMA (30 mg, Mn: 7200, PDI:1.44; 0.0042 mmol), AIBN (0.17 mg; 0.0011 mmol) and PEGMA ((Mn=475 n= 7-8; 0.5 M; 97.3 mg; 0.21 mmol) were dissolved in dioxane (420 μL) at a [monomer]/[macroRAFT agent]/[initiator] mole ratio of 50/1/0.25. The reaction mixture was then divided into equal amounts and transferred to vials. Each vial was degassed with nitrogen for about 15 minutes. The samples were then immersed into an oil bath at 65ºC. The polymerization was allowed to run for 0.5 h, 1 h, 2 h, and 4 h. After ^{1}H-NMR analysis of the reaction medium for determination of monomer conversion (Equation 3.1), the reaction mixtures were purified by dissolving in dioxane and precipitated in hexane five times. ^{1}H-NMR and GPC analyses of purified samples were performed to characterize copolymers.

^{1}H NMR (CDCl3): δ in ppm: 2.41 (2H, br s), 1.38 (3H, br d), 1.90 (3H, br d), 0.85 (2H, br d)

In a typical copolymerization procedure where PPEGMA was used as a macroRAFT agent, the above-given procedure was repeated using PPEGMA (Mn: 7600, PDI:1.15) as a macroRAFT agent instead of PPFMA. All polymerization and purification conditions were kept the same with those given above.

3.3.5. Postpolymerization Modification of P(PFMA) with Arginine Methyl Ester

First of all, arginine methyl ester.dihydrochloride (AME) (417.6 mg; 1.6 mmol) and TEA (484 mg; 666 μL; 4.8 mmol) were mixed together in dry DMF (2332 μL) in order to remove the TEA-chloride salt formed as a precipitate. Separately, PPFMA (200 mg; repeating unit Mw: 252 g/mol; 0.8 mmol repeating unit) was dissolved in dry DMF (1.5 mL). The needed amount of AME-TEA solution was then added (either rapidly or drop-by-drop) to the polymer solution to yield a PPFMA/AME/TEA mol ratio of 1/1/3. The reaction was allowed to stir at 50^{o}C for 16 h.

DMF was then removed from the reaction mixture by vacuum oven. To investigate the reaction yield, the reaction mixture was first analyzed by ^{19}F-NMR. It was then dissolved in water and extracted into diethyl ether 4 times. Both phases were investigated using ^{1}H-NMR. The water phase which contained the desired product, i.e. arginine-modified PPFMA, was collected and then dialyzed against acidic water for 3 days using a dialysis tubing with a MWCO of 1000 Da. The final product was obtained after freeze-drying.

^{1}H NMR ($CDCl_3$): δ in ppm: 3.66-3.23 (3H, m), 3.11 (2H, t), 1.80-1.50 (9H, m)

Modification reaction yield was calculated according to Equation 3.3 using ^{19}F-NMR data of reaction solution mixture before purification.

$$Reaction\ Yield = \frac{\int Product}{\int Product + \int Starting\ Material} \qquad (3.3)$$

3.3.6. Agarose Gel Electrophoresis Method

To determine DNA complexation of AME modified PPFMA, polymers were complexed with 681 b.p. DNA at different N^+/P^- ratios (1/1, 2/1, 5/1, 10/1, 20/1, 50/1, 100/1, 200/1). Polymers (Mn: 8000) were dissolved in phosphate buffer solution and mixed with DNA solution in Tris-EDTA buffer (21 ng/µL, 2.36µL). Polymer and DNA samples were incubated at room temperature for 15 min. The gel was run at 100 V for 25 min.

CHAPTER 4

RESULTS AND DISCUSSION

4.1. PFMA Synthesis

In this work, it is intended to synthesize arginine containing polymers for potential intracellular drug delivery applications. For this purpose, an active ester monomer, PFMA was synthesized, polymerized and then modified with arginine methyl ester. It is known from literature that activated ester polymers are quite selective for reactions with amines (Theato 2008). PPFMA was chosen because of its advantages over other activated ester polymers such as high-hydrolytic stability, improved solubility, high reaction efficiency and selectivity (Gibson, Fröhlich et al. 2009). Accordingly, PFMA monomer was first synthesized as an initial compound for this thesis research. The PFMA synthesis procedure was adapted from a previous report (Eberhardt, Mruk et al. 2005).

For the synthesis of PFMA monomer, pentafluorophenol was reacted with methacryloyl chloride in DCM. The synthesis step was followed by various purification steps including extraction in water-DCM to remove methacrylic acid formed, vacuum-distillation to remove unconverted pentafluorophenol, and basic alumina column chromatography to remove residual methacrylic acid.

Figure 4.1. shows the ^{1}H-NMR spectrum of PFMA monomer after vacuum distillation. According to this spectrum, PFMA monomer synthesis was successful. However, the chemical shifts at 6.23 ppm (1H), 5.82 ppm (1H) and 2.01 ppm (3H) show the presence of methacrylic acid (MAA) monomer. To further purify monomer, column chromatography was done using aluminum oxide to remove residual methacrylic acid. Positively charged alumina holds methacrylic acid monomer and only PFMA monomer leaves the column. According to the NMR spectrum of the monomer collected after column chromatography (Figure 4.2), pure PFMA monomer was obtained successfully. ^{19}F-NMR result was taken in order to be sure about the structure of PFMA and can be seen in Appendix A (Figure A 1).

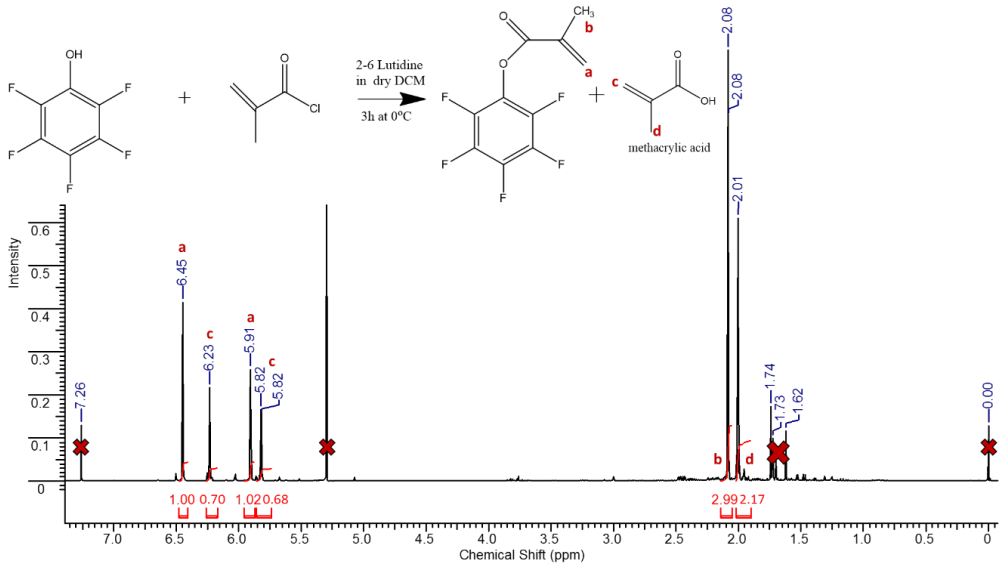

Figure 4.1. ^{1}H-NMR spectrum of PFMA monomer after vacuum distillation

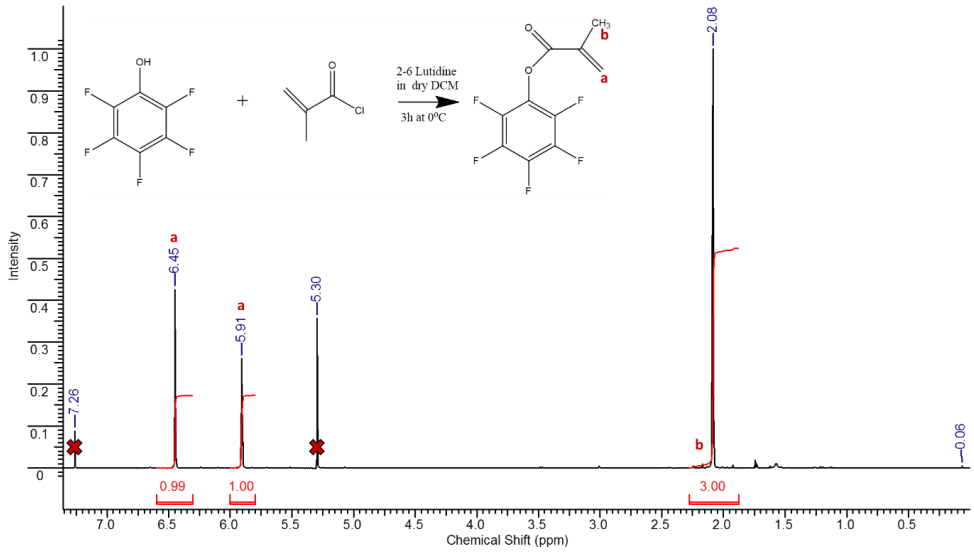

Figure 4.2. ^{1}H-NMR spectrum of PFMA monomer after column chromatography

After the synthesis of PFMA monomer, RAFT polymerization kinetics of PFMA was investigated, as described in the next section.

4.2. RAFT Polymerization of PFMA

In order to synthesize well-defined PFMA polymers, polymerizations at varying PFMA/RAFT/Initiator mol ratios and temperatures were performed as summarized in Table 3.1.

Figure 4.3 shows monomer conversion versus time graphs of RAFT polymerizations of PFMA performed at varying monomer/RAFT agent/initiator mol ratios and polymerization temperatures. Y axis shows monomer consumption (in other words polymer synthesis) at a specific time. When monomer consumption is plotted versus time, relationship is expected to be linear according to the RAFT controlled mechanism theory. This indicates the presence of constant radical source during polymerization which is in accord with RAFT polymerization mechanism. Based on the coefficients of determination (or correlation coefficients squared) calculated from the lines of best fits to the collected data, the polymerization performed at a [M]/[RAFT]/[AIBN] molar ratio of 25/1/0.125 and 80°C shows the poorest RAFT-mechanism controlled character among the conditions tested. Other conditions tested showed R^2 values higher than 0.95, suggesting RAFT controlled character of polymerizations. With the decreasing temperature (comparison of 25/1/0.25 at 90^{o}C and 25/1/0.25 at 80^{o}C) the monomer conversion was found to decrease slightly. This was attributed to the slower initiation step at lower temperatures.

As it can be seen in the number average molecular weight (Mn) versus monomer conversion, and the molecular weight distribution (Mw/Mn) versus monomer conversion graphs in Figure 4.4, controlled molecular weight polymers of PFMA with narrow molecular weight distribution (lower than 1.4) were synthesized. High PDI values suggest the slight presence of side reactions such as branching and/or slow fragmentation of the RAFT agent. Linear relation between Mn and conversion, indicates RAFT controlled character of polymerizations. (Figure 4.4). This relation is explained by theory (Equation 3.2) that a linear relationship between conversion and molecular weight of RAFT controlled polymers. Decreasing the monomer to RAFT ratio ([M]/[R] ratio) in polymerization medium decreased the molecular weight of polymers as expected, since the Mn of RAFT synthesized polymers is linearly dependent on the ([M]/[R] ratio as it can be seen from Equation 3.2. Moreover, the molecular weight of polymers formed at lower temperature was lower than that of

polymers formed at 90°C. For polymerizations performed at 100/1/0.25 ratio and 90°C, polymers having wide molecular weight distributions were obtained. This indicates the presence of side reactions at high ([M]/[R] ratio, possibly leading to some degree of branching.

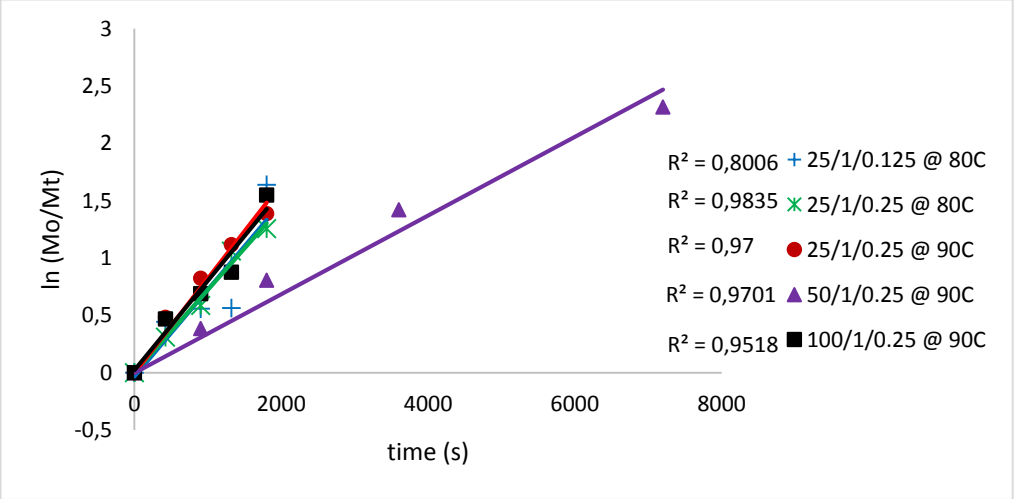

Figure 4.3. Ln Mo/M versus polymerization time for RAFT polymerizations of PFMA performed at varying monomer/RAFT agent/initiator mol ratios and polymerization temperatures. Mo and M refer to initial concentration of the monomer and monomer concentration at a specific time

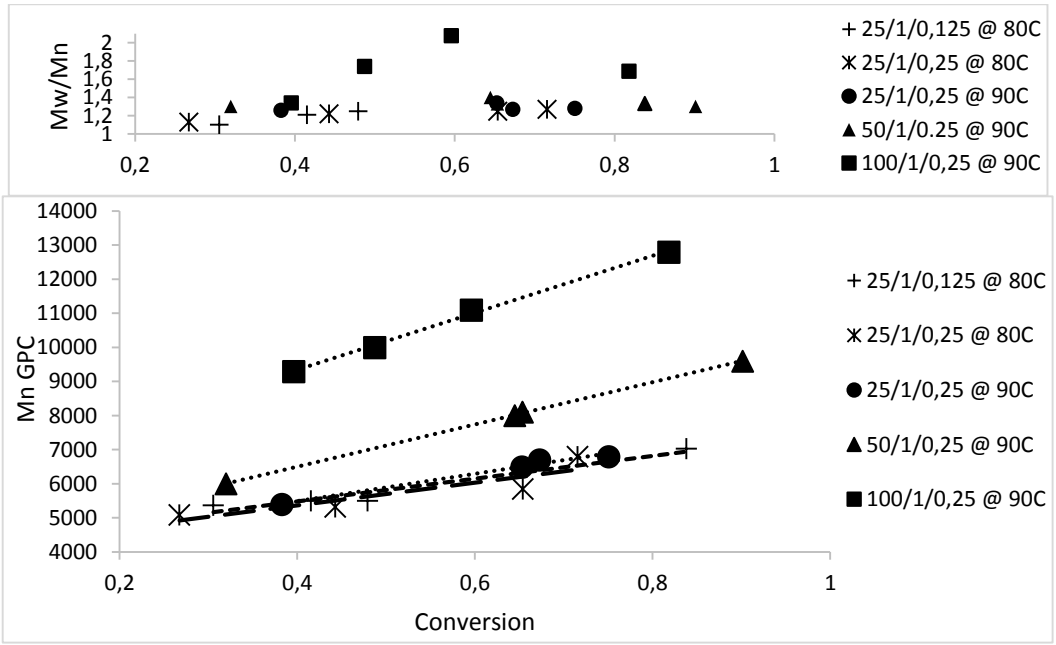

Figure 4.4. Kinetic plots of PFMA RAFT polymerization

Polymerization results are summarized in Table B 1. Monomer conversions were calculated from Equation 3.1 by taking the ratio of methylene group protons of polymer backbone (at 2.4 ppm) to the sum of methylene group protons of both monomer (at 5.90 ppm and polymer at 2.4 ppm) (Figure B 1). Mn (NMR) was calculated according to Equation 3.2 using integration values of RAFT end-group protons at 7.3-7.9 ppm and repeating polymer two proton units at 2.41 ppm. Degree of polymerization (PD) was calculated from Equation 3.4. PDI and Mn values were directly taken from GPC analysis results. The representative GPC chromatograms of 25/1/0.25 at 90°C polymerization are also shown in Figure B 3.

$$Degree\ of\ Polymerization = \frac{(\int_{2,41} Polymer)/2}{(\int_{7,3-7,9} RAFT)/5} \quad (4.1)$$

4.3. Synthesis of P(PFMA)-*b*-P(PEGMA) and P(PEGMA)-*b*-(PPFMA)

In this part of the thesis, block copolymerization of PFMA and PEGMA was investigated. The aim of copolymerizing PFMA with PEGMA is to add a biocompatible, hydrophilic, neutral polymer component to the system, considering the possible use of arginine modified PFMA polymers for electrostatic complexation with nucleic acid therapeutics. Block copolymerization of PFMA and PEGMA via RAFT mechanism has not been reported yet in literature. Optimization experiments were therefore needed. Two different macroRAFT agents, PPFMA and PPEGMA, were utilized separately for block copolymerizations to test their chain extension abilities. The PDI and molecular weight of macroCTA together with chemical structure have influence on the chain extension ability of macroRAFT agents. PPEGMA synthesis was described in Chapter 3. ^{1}H-NMR result and characterization of PPEGMA are given in Figure C1. In both types of chain extension copolymerization experiments, a [monomer]/[RAFT agent]/[initiator] ratio of 50/1/0.25 was used. In copolymerizations performed using PPFMA as a macroRAFT agent, the concentration of PEGMA monomer was adjusted to 0.5 M considering the relatively low solubility of PEGMA in dioxane. The GPC chromatograms of both copolymerizations are shown in Figure 4.5.

The Mn values and molecular weight distributions of the copolymers obtained are shown in Figure 4.6. As seen in the results, the linear increase in Mn indicated that the chain extension block copolymerizations were successfully performed using both macroRAFT agents. Relatively larger PDI values of (PFMA)-co-P(PEGMA) copolymers were attributed to the larger PDI value of the PPFMA macroRAFT agent.

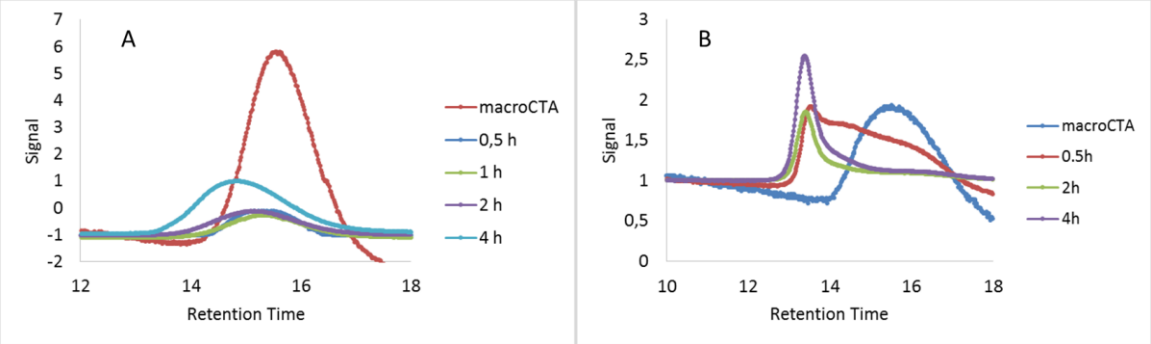

Figure 4.5. GPC results of A:P(PFMA)-co-P(PEGMA) and B:P(PEGMA)-co-P(PFMA) (0.5 M [50/1/0.25])

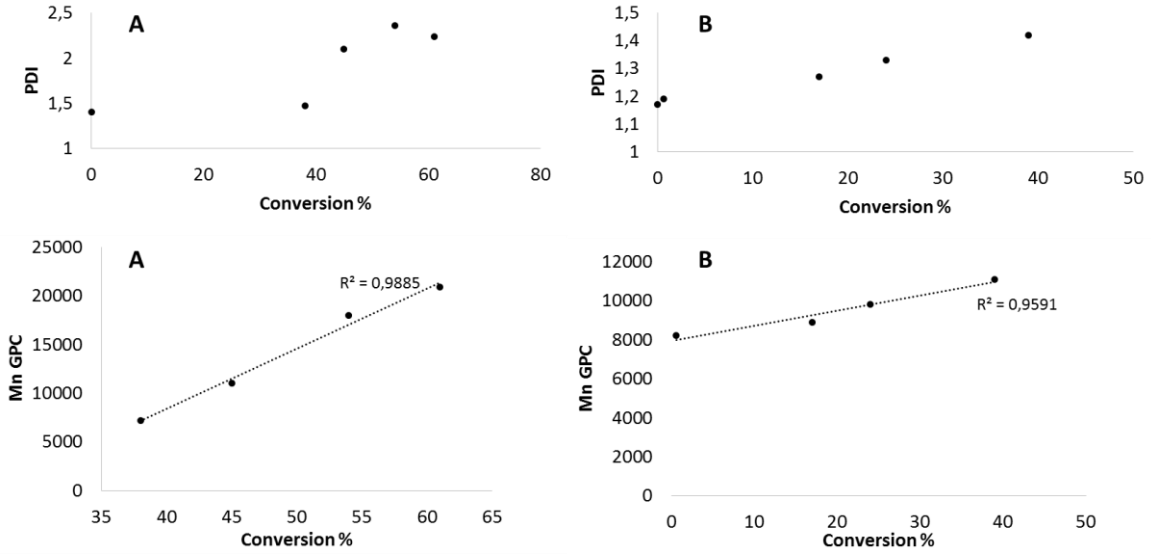

Figure 4.6. Kinetic plots of chain extension copolymerizations A:P(PFMA)-co-P(PEGMA) and B:P(PEGMA)-co-P(PFMA) ([M]=0.5 M; [M]/[R]/[I] mol ratio=[50/1/0.25])

4.4. Arginine Methyl Ester and PFMA Reaction

PFMA polymers were modified with arginine methyl ester (AME) using the protocol given in Chapter 3. The results of optimization experiments of the modification showed that dry solvent usage, slow addition of AME into the polymer solution and the stoichiometric ratios of the reagents are the key parameters to obtain high modification reaction yield (Equation 3.3, Chapter 3). All reaction mixtures were investigated by ^{19}F-NMR analysis before purification to calculate the modification yield of PFMA units with AME (Figure D1). The complete modification of PFMA units with arginine, meaning 100% modification yield obtained only when a PFMA repeating units/AME/TEA mol ratio of 1/1/3 was used. Table D 1 shows the different reagent ratios tested and the modification yields obtained. Reaction scheme is given in Figure 4.7.

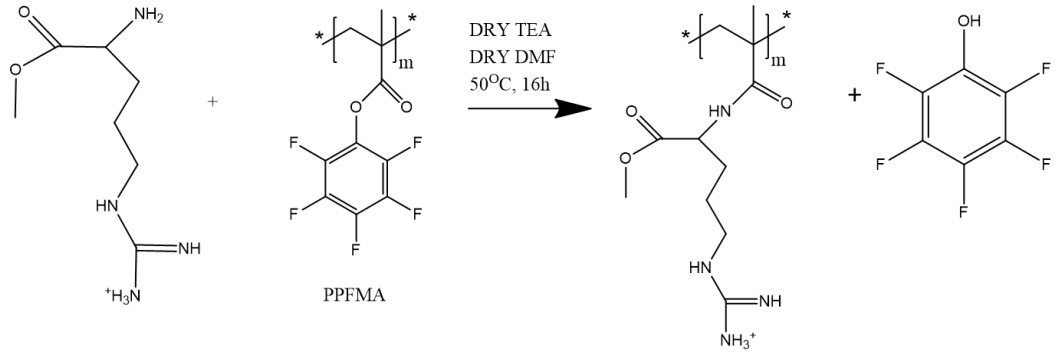

Figure 4.7. Scheme of PPFMA modification with AME

Upon determination of modification yields, the reaction mixtures were dissolved in water and extracted with diethyl ether (DEE). The NMR analyses of both phases indicated the presence of AME-modified PFMA in water phase and unmodified polymer and side product penrafluorophenol in DEE phase. Figures 4.8, 4.9 and 4.10 show the ^{1}H NMR spectra of AME and AME-modified polymer obtained using a PFMA/AME/TEA mol ratio of 1/2/2 and 1/1/3, respectively. When the spectra of AME and AME-modified polymer are compared (Figures 4.8 and 4.9), one can see clearly the signal shift of -C**H** adjacent to primary amine at 4.08 ppm to 3.62 ppm upon reaction of amine with pentafluorophenyl group of polymer forming an amide bond. The signal of

protons of methyl ester group also shifts from 3.73 ppm to 3.63 ppm upon reaction of amine with PPFMA. It is clear from the integrations in the spectrum in Figure 4.9 that the modification yield of the polymer was only 41% and there was unconjugated AME in the medium when PFMA/AME/TEA mol ratio was 1/2/2.

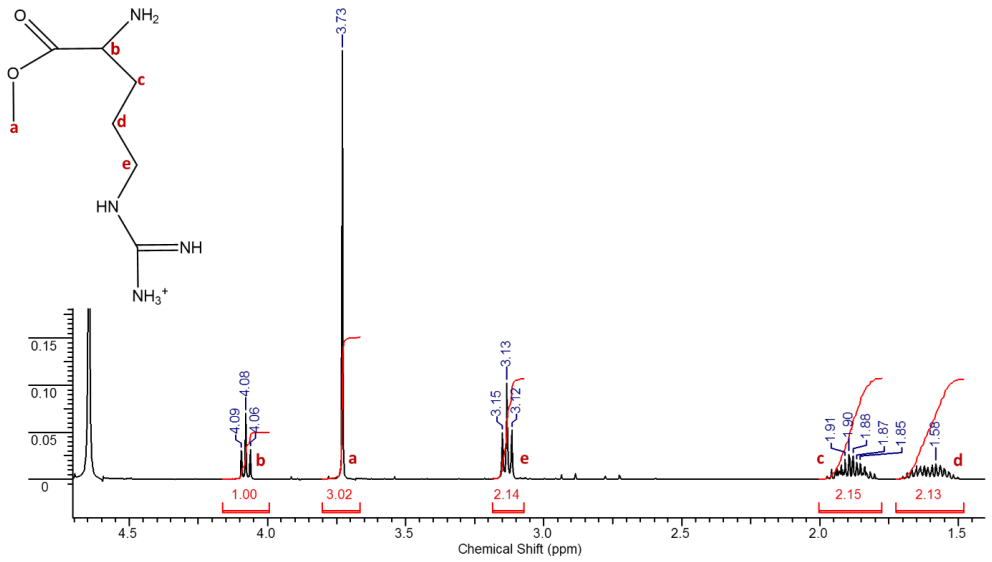

Figure 4.8. ^{1}H-NMR result of AME in D_2O

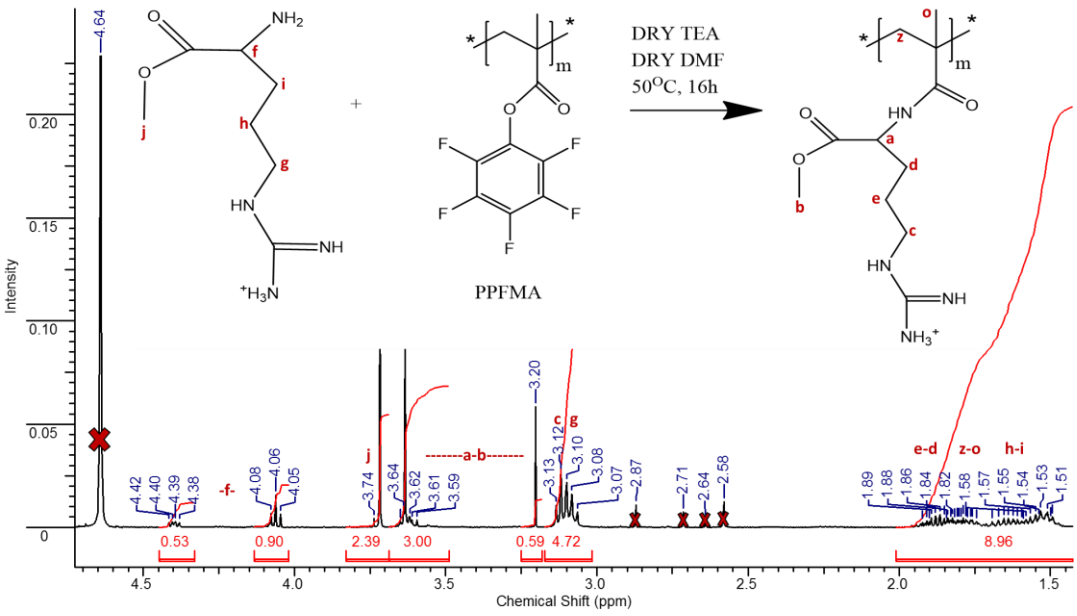

Figure 4.9. ^{1}H-NMR spectrum of AME modified PPFMA after purification (in D_2O) (PPFMA/AME/TEA mol ratio: 1/2/2)

When PFMA/AME/TEA mol ratio was 1/1/3 and also AME solution was added to the polymer solution drop wise, the modification yield reached to 100% (Figure 4.10). Free AME was not present in the spectrum in Figure 4.10. ^{19}F-NMR analysis result also supported the results obtained by ^{1}H-NMR analysis (Figure 4.11). In the ^{19}F-NMR spectrum of the reaction mixture, 100% conversion of pentafluorophenyl groups on the polymer to pentafluorophenol groups can be clearly seen. Furthermore, the removal of pentafluorophenyl groups on the polymer upon modification with AME and purification was also observed via UV-Vis spectroscopy (Figure 4.12).

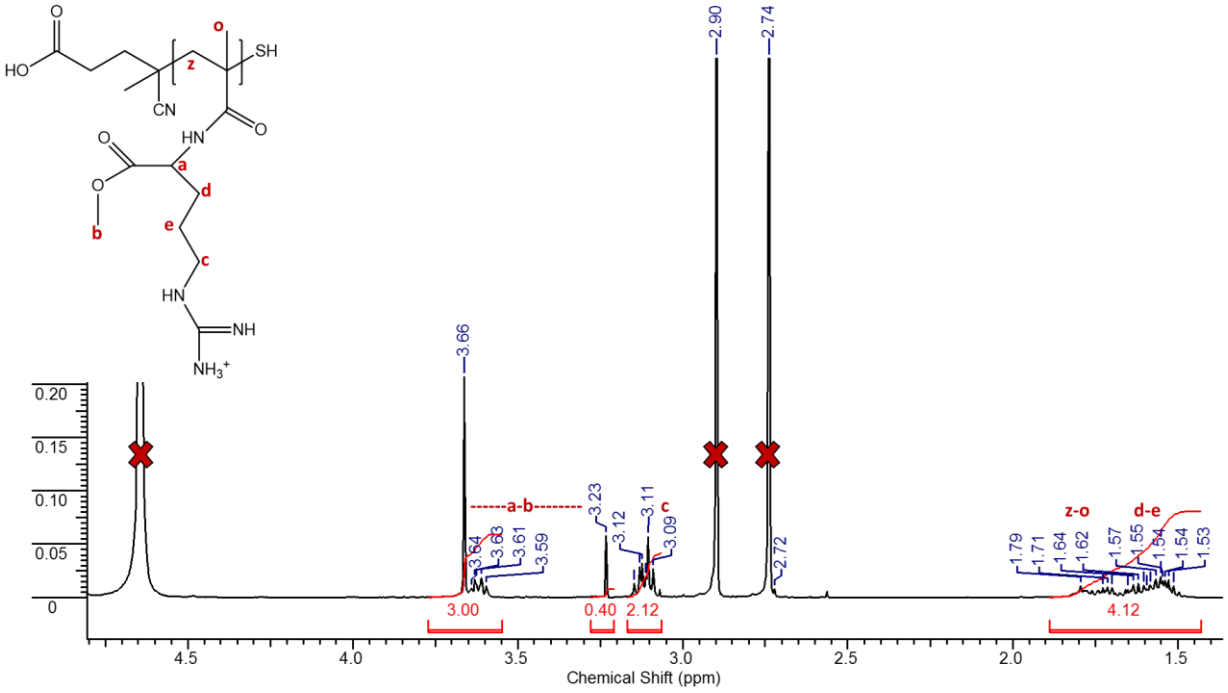

Figure 4.10. ^{1}H-NMR spectrum of AME modified PPFMA after purification (in D_2O) (PPFMA/AME/TEA mol ratio: 1/1/3)

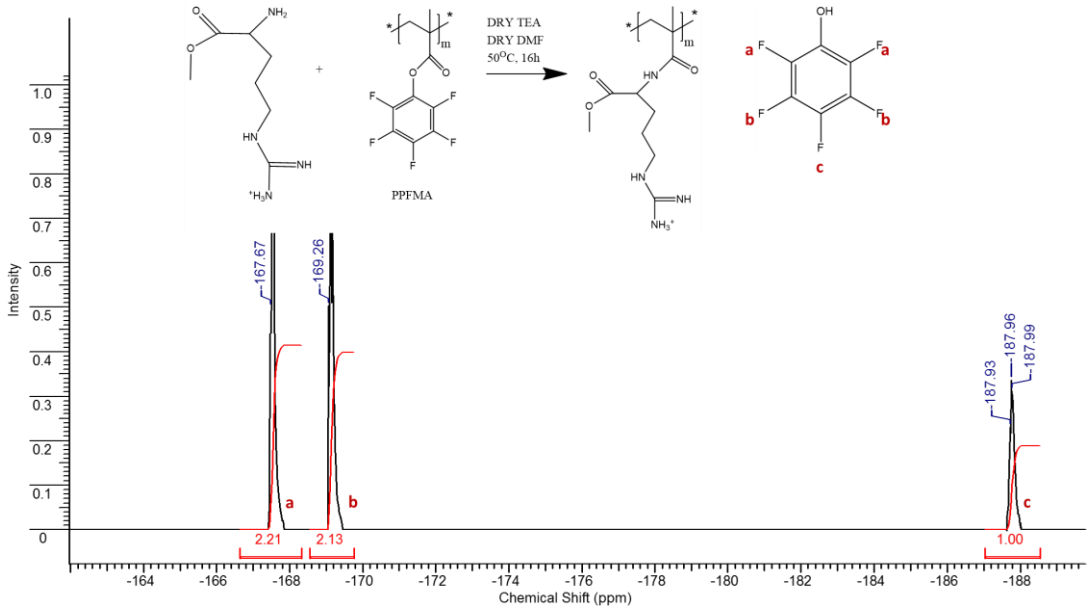

Figure 4.11. ^{19}F-NMR spectrum of the reaction mixture before purification (PPFMA/AME/TEA mol ratio: 1/1/3)

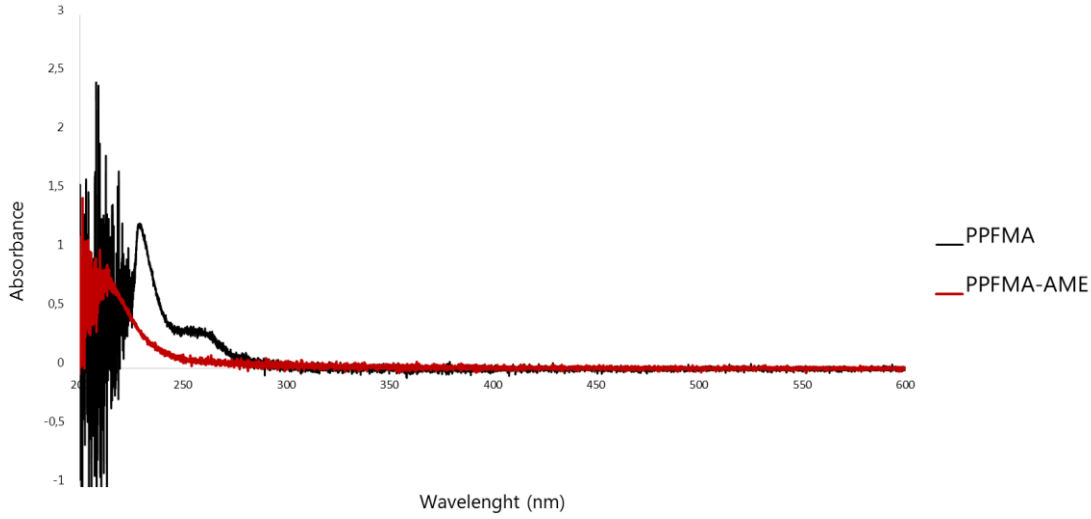

Figure 4.12. UV-vis spectra of PPFMA before and after modification with AME (PPFMA/AME/TEA: 1/1/3)

4.5. DNA Complexation of DNA with AME-modified PPFMA

Complexation of DNA with arginine modified polymer was performed based on electrostatic interactions between negatively charged phosphate groups of DNA and positively charged guanidine group of arginine. The complexation was carried out at varying guanidine/phosphate ratios (N/P) as shown in Figures 4.13 and 4.14. The complexation was verified by gel electrophoresis. Polyplex formation was expected to occur after addition of DNA to arginine modified polymer. According to gel electrophoresis data, complexation of all DNA molecules with AME modified PPFMA was achieved at a N/P ratio of 200/1, as indicated by the complete disappearance of free DNA band on the gel. It was also observed that with increasing N/P ratios, the intensity of free DNA band gradually decreased, suggesting increasing number of DNA molecules complexing with positively charged polymer.

DNA polyplex formation was also investigated via DLS measurements (Figure 4.15). The DLS measurements showed the hydrodynamic diameter (D_h) of DNA before and after addition of AME-modified polymer was 109 and 58 nm, respectively, suggesting the condensation of DNA by the positively charged polymers. To improve the biocompability of polyplexes, a hydrophilic, neutral polymer block such as PPEGMA can be added to PPFMA. This would the focus of future studies, as it is out of the scope of this thesis research.

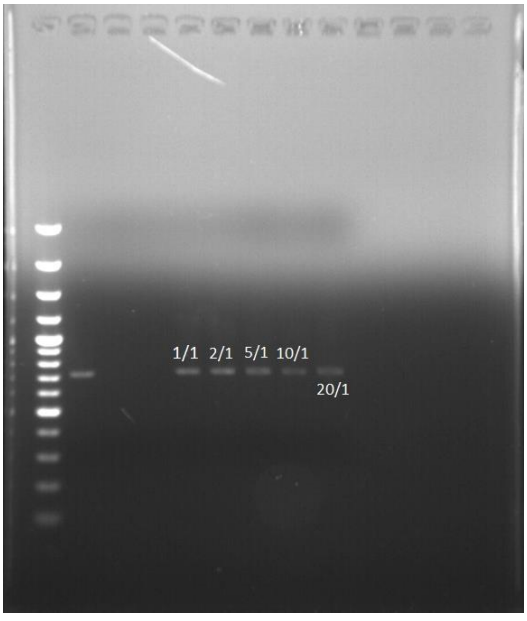

Figure 4.13. Complexation of DNA (681 bp) with AME-modified polymer at varying N/P ratios (1/1; 2/1; 5/1; 10/1; 20/1)

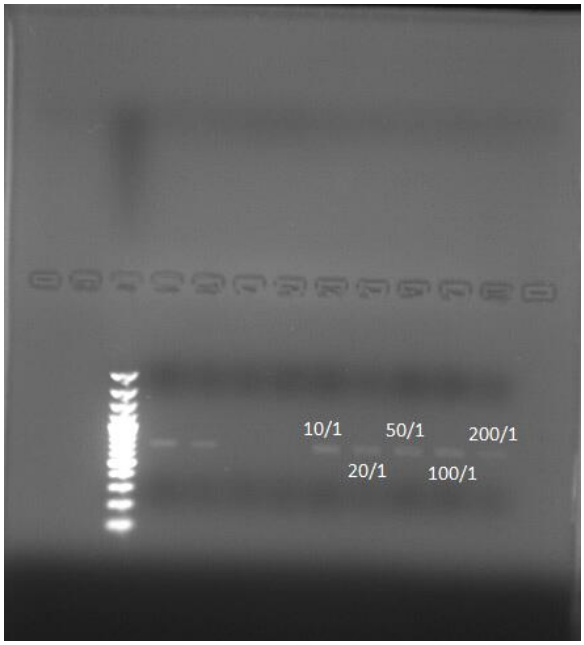

Figure 4.14. Complexation of DNA (681 bp) with AME-modified polymer at varying N/P ratios (10/1; 20/1; 50/1; 100/1; 200/1)

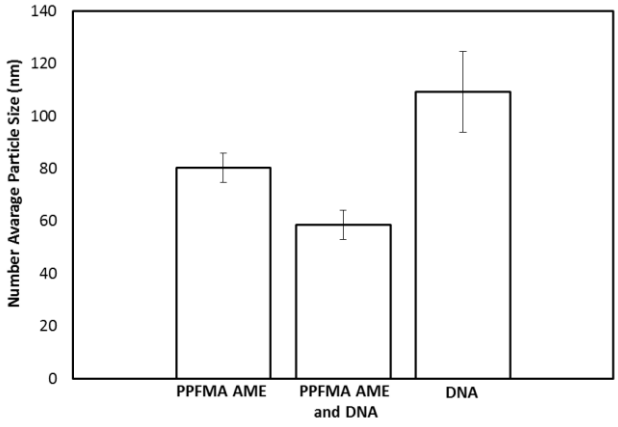

Figure 4.15. DLS measurements of AME-modified polymer and free DNA (681 bp) before and after complexation with polymer at a N/P ratio of 200/1

CHAPTER 5

CONCLUSION

In this work, well-defined arginine containing polymers have been generated as potential components of intracellular delivery systems for DNA-based therapeutics and the potential of these polymers was briefly investigated via preliminary DNA complexation experiments. Pentafluorophenyl methacrylate (PFMA) monomer was chosen as an amine-reactive monomer considering its high reactivity and selectivity against primary amines. Polymerization experiments revealed the successful synthesis of well-defined PFMA polymers via RAFT-controlled polymerization mechanism. The linear relationship between the monomer conversions and polymers molecular weights proved the RAFT-controlled mechanism. Block copolymerization of PFMA with polyethyleneglycol methylether methacrylate (PEGMA) was also shown. PEGMA was chosen as a comonomer to improve the biocompatibility of arginine-containing polymer block for possible use of the polymers in drug delivery area. Block copolymerization was achieved by using PPFMA or PPEGMA as a macroCTA, as indicated by GPC measurements.

PPFMA was modified with arginine methylester (AME). In optimization experiments, it was determined that dry solvent usage, slow addition of AME into the polymer solution and the stochiometric ratios of the reagents are the key parameters to obtain high modification yield. The complete modification of PFMA units with arginine, meaning 100% modification yield obtained only when a PFMA/AME/TEA mol ratio of 1/1/3 was used and AME was added slowly into the polymer solution.

The final step of the study was to investigate the DNA complexation ability of arginine-modified polymer. Gel electrophoresis results indicated that the polymer was able to form electrostatic complexes with DNA completely at a guanidine/phosphate ratio of 200/1. The DLS measurements showed the formation of polyplex particles and condensation of DNA. The D_h of free DNA and polyplexes was found to be 109 and 58 nm, respectively.

This study can be improved by further investigations. The effect of arginine containing polymer on cell viability has to be investigated. Accordingly, uptake

mechanism and intracellular distribution of arginine containing polymer can be further investigated. Separately, conditions for RAFT polymerization of PFMA and block copolymerization with PEGMA can be further optimized to obtain polymers with better controlled characteristics. Finally, block copolymers of PFMA and PEGMA can be modified with AME to obtain double hydrophilic, arginine containing copolymers. The DNA complexation ability and cell culture studies of these copolymers can be investigated.

REFERENCES

Batz, H. G., Franzmann, G., & Ringsdorf, H. (1972). Model reactions for synthesis of pharmacologically active polymers by way of monomeric and polymeric reactive esters. *Angewandte Chemie International Edition in English*, *11*(12), 1103-1104.

Beija, M., Li, Y., Lowe, A. B., Davis, T. P., & Boyer, C. (2013). Factors influencing the synthesis and the post-modification of PEGylated pentafluorophenyl acrylate containing copolymers. *European Polymer Journal*, *49*(10), 3060-3071.

Boyer, C., Bulmus, V., Davis, T. P., Ladmiral, V., Liu, J., & Perrier, S. (2009). Bioapplications of RAFT polymerization. *Chemical reviews*, *109*(11), 5402-5436.

Carrasco, L. (1994). Entry of animal viruses and macromolecules into cells. *FEBS letters*, *350*(2), 151-154.

Cohen, J. L., Almutairi, A., Cohen, J. A., Bernstein, M., Brody, S. L., Schuster, D. P., & Fréchet, J. M. (2008). Enhanced cell penetration of acid-degradable particles functionalized with cell-penetrating peptides. *Bioconjugate chemistry*, *19*(4), 876-881.

Eberhardt, M., Mruk, R., Zentel, R., & Théato, P. (2005). Synthesis of pentafluorophenyl (meth) acrylate polymers: New precursor polymers for the synthesis of multifunctional materials. *European Polymer Journal*, *41*(7), 1569-1575.

Ferruti, P., Bettelli, A., & Feré, A. (1972). High polymers of acrylic and methacrylic esters of< i> N</i>-hydroxysuccinimide as polyacrylamide and polymethacrylamide precursors. *Polymer*, *13*(10), 462-464.

Fonseca, S. B., Pereira, M. P., & Kelley, S. O. (2009). Recent advances in the use of cell-penetrating peptides for medical and biological applications. *Adv Drug Deliv Rev*, *61*(11), 953-964.

Futaki, S. (2005). Membrane-permeable arginine-rich peptides and the translocation mechanisms. *Adv Drug Deliv Rev*, *57*(4), 547-558. doi: 10.1016/j.addr.2004.10.009

Gibson, M. I., Fröhlich, E., & Klok, H.-A. (2009). Postpolymerization modification of poly(pentafluorophenyl methacrylate): Synthesis of a diverse water-soluble polymer library. *Journal of Polymer Science Part A: Polymer Chemistry*, *47*(17), 4332-4345. doi: 10.1002/pola.23486

Gregory, A., & Stenzel, M. H. (2012). Complex polymer architectures via RAFT polymerization: From fundamental process to extending the scope using click

chemistry and nature's building blocks. *Progress in Polymer Science, 37*(1), 38-105.

Han, S.-o., Mahato, R. I., Sung, Y. K., & Kim, S. W. (2000). Development of biomaterials for gene therapy. *Molecular Therapy, 2*(4), 302-317.

Herce, H., Garcia, A., Litt, J., Kane, R., Martin, P., Enrique, N., . . . Milesi, V. (2009). Arginine-rich peptides destabilize the plasma membrane, consistent with a pore formation translocation mechanism of cell-penetrating peptides. *Biophysical journal, 97*(7), 1917-1925.

Katayama, S., Hirose, H., Takayama, K., Nakase, I., & Futaki, S. (2011). Acylation of octaarginine: Implication to the use of intracellular delivery vectors. *J Control Release, 149*(1), 29-35. doi: 10.1016/j.jconrel.2010.02.004

Kim, T.-i., Baek, J.-u., Yoon, J. K., Choi, J. S., Kim, K., & Park, J.-s. (2007). Synthesis and characterization of a novel arginine-grafted dendritic block copolymer for gene delivery and study of its cellular uptake pathway leading to transfection. *Bioconjugate chemistry, 18*(2), 309-317.

Liechty, W. B., Kryscio, D. R., Slaughter, B. V., & Peppas, N. A. (2010). Polymers for drug delivery systems. *Annual review of chemical and biomolecular engineering, 1*, 149.

Lindgren, M., Hällbrink, M., Prochiantz, A., & Langel, Ü. (2000). Cell-penetrating peptides. *Trends in pharmacological sciences, 21*(3), 99-103.

Liu, B. R., Huang, Y. W., Winiarz, J. G., Chiang, H. J., & Lee, H. J. (2011). Intracellular delivery of quantum dots mediated by a histidine- and arginine-rich HR9 cell-penetrating peptide through the direct membrane translocation mechanism. *Biomaterials, 32*(13), 3520-3537. doi: 10.1016/j.biomaterials.2011.01.041

Madani, F., Lindberg, S., Langel, Ü., Futaki, S., & Gräslund, A. (2011). Mechanisms of cellular uptake of cell-penetrating peptides. *Journal of Biophysics, 2011*.

Mudhakir, D., & Harashima, H. (2009). Learning from the viral journey: how to enter cells and how to overcome intracellular barriers to reach the nucleus. *The AAPS journal, 11*(1), 65-77.

Murthy, N., Campbell, J., Fausto, N., Hoffman, A. S., & Stayton, P. S. (2003). Bioinspired pH-responsive polymers for the intracellular delivery of biomolecular drugs. *Bioconjugate chemistry, 14*(2), 412-419.

Nakase, I., Konishi, Y., Ueda, M., Saji, H., & Futaki, S. (2012). Accumulation of arginine-rich cell-penetrating peptides in tumors and the potential for anticancer drug delivery in vivo. *J Control Release, 159*(2), 181-188. doi: 10.1016/j.jconrel.2012.01.016

Nuhn, L., Hirsch, M., Krieg, B., Koynov, K., Fischer, K., Schmidt, M., . . . Zentel, R. (2012). Cationic nanohydrogel particles as potential siRNA carriers for cellular delivery. *ACS nano, 6*(3), 2198-2214.

Piantavigna, S., McCubbin, G. A., Boehnke, S., Graham, B., Spiccia, L., & Martin, L. L. (2011). A mechanistic investigation of cell-penetrating Tat peptides with supported lipid membranes. *Biochimica et Biophysica Acta (BBA)-Biomembranes, 1808*(7), 1811-1817.

Smith, A. E., & Helenius, A. (2004). How viruses enter animal cells. *Science, 304*(5668), 237-242.

Stenzel, M. H. (2008). RAFT polymerization: an avenue to functional polymeric micelles for drug delivery. *Chem Commun (Camb)*(30), 3486-3503.

Stewart, K. M., Horton, K. L., & Kelley, S. O. (2008). Cell-penetrating peptides as delivery vehicles for biology and medicine. *Org. Biomol. Chem., 6*(13), 2242-2255.

Theato, P. (2008). Synthesis of well-defined polymeric activated esters. *Journal of Polymer Science Part A: Polymer Chemistry, 46*(20), 6677-6687. doi: 10.1002/pola.22994

Treat, N. J., Smith, D., Teng, C., Flores, J. D., Abel, B. A., York, A. W., . . . McCormick, C. L. (2011). Guanidine-Containing Methacrylamide (Co) polymers via a RAFT: Toward a Cell-Penetrating Peptide Mimic. *ACS macro letters, 1*(1), 100-104.

Vasant V. Ranade, J. B. C. (2011). *Drug Delivery Systems*: CRC Press.

Veiseh, O., Kievit, F. M., Mok, H., Ayesh, J., Clark, C., Fang, C., . . . Zhang, M. (2011). Cell transcytosing poly-arginine coated magnetic nanovector for safe and effective siRNA delivery. *Biomaterials, 32*(24), 5717-5725. doi: 10.1016/j.biomaterials.2011.04.039

Wang, C., Cheng, L., Xu, H., & Liu, Z. (2012). Towards whole-body imaging at the single cell level using ultra-sensitive stem cell labeling with oligo-arginine modified upconversion nanoparticles. *Biomaterials, 33*(19), 4872-4881.

Zorko, M., & Langel, Ü. (2005). Cell-penetrating peptides: mechanism and kinetics of cargo delivery. *Adv Drug Deliv Rev, 57*(4), 529-545.

APPENDIX A

SYTHESIS OF PFMA MONOMER

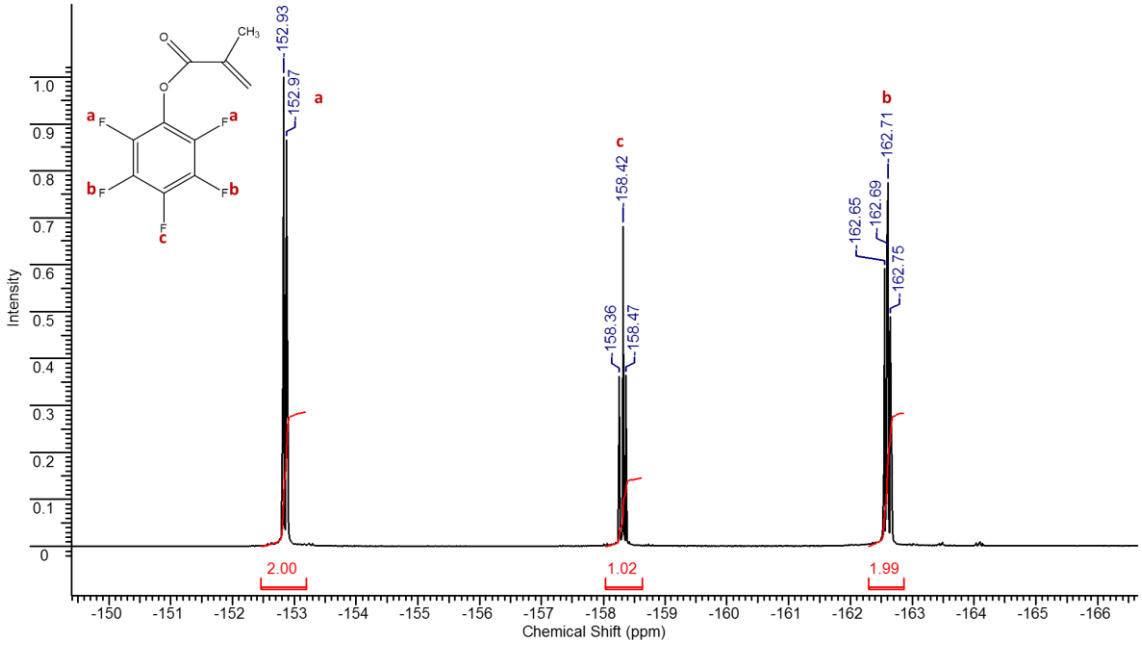

Figure A 1. ^{19}F-NMR result of synthesized PFMA after column chromatography

APPENDIX B

PFMA RAFT POLYMERIZATION

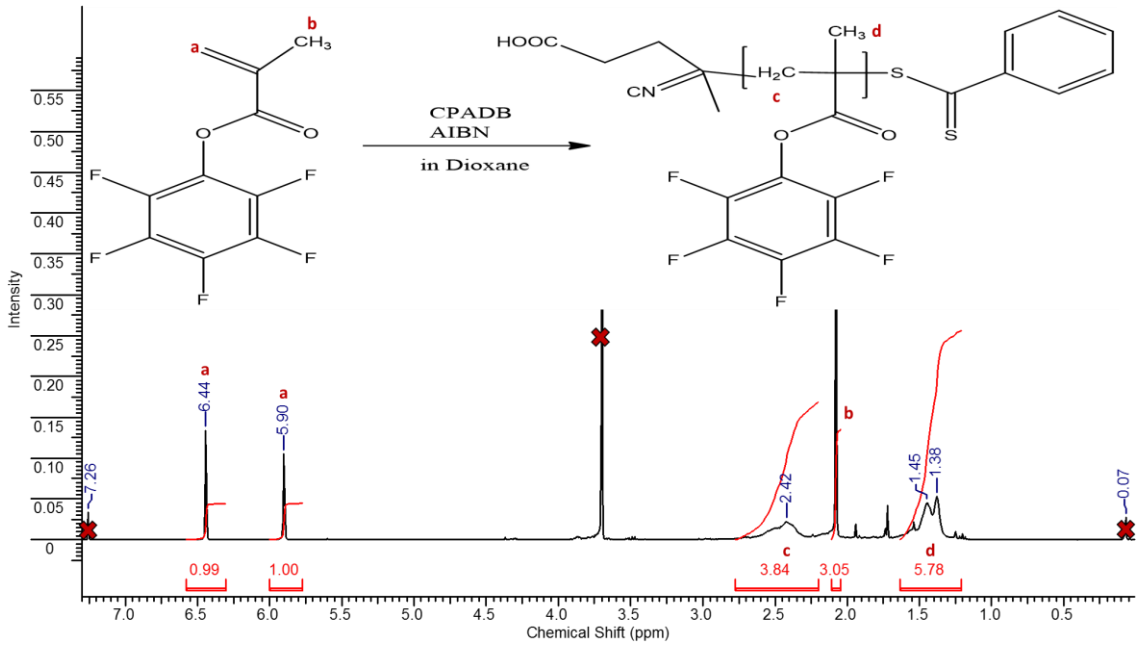

Figure B 1. ^{1}H-NMR result of PFMA RAFT polymerization before purification (Monomer Concentration: 2M and [M]/[R]/[I]: 25/1/0.25 at 90^{o}C)

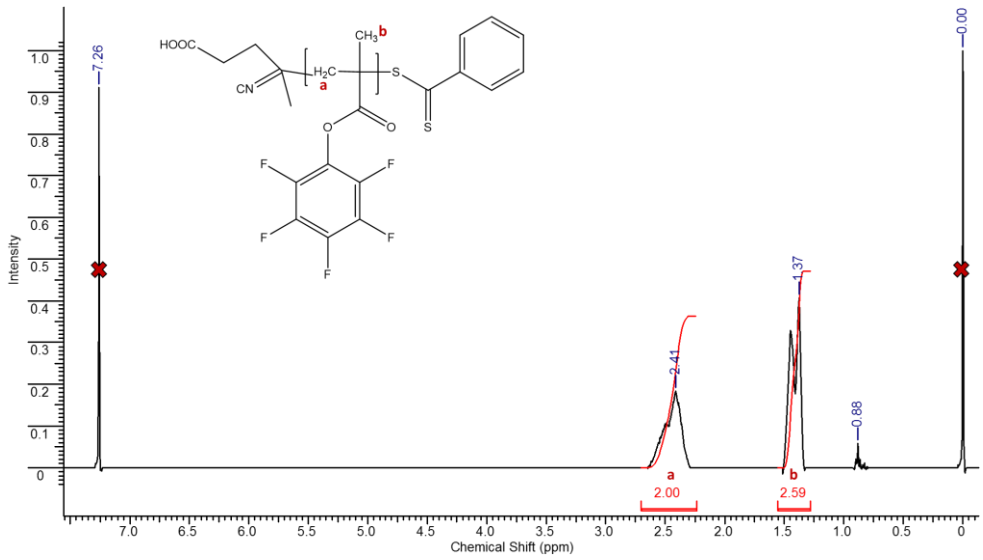

Figure B 2. ^{1}H-NMR result of PFMA RAFT polymerization after purification (Monomer Concentration: 2M and [M]/[R]/[I]: 25/1/0.25 at 90^{o}C)

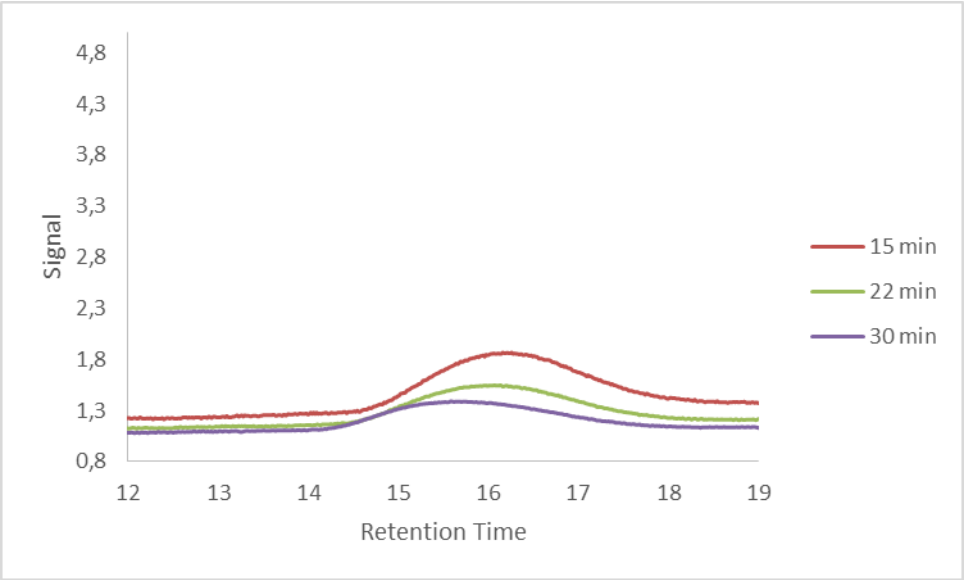

Figure B 3. GPC result of PFMA RAFT polymerization after purification (Monomer Concentration: 2M and [M]/[R]/[I]: 25/1/0.25 at 90ºC)

Table B 1. Results of PFMA Polymerization

[M]/[R]/[I]	Time (min)	Conversion	Mn Theo	PD	Mn GPC	PDI	Mn ^{1}H-NMR
50/1/0.25	15	0.32	4307	23	6000	1.3	4834
50/1/0.25	30	0.55	8403	31	8000	1.4	8164
50/1/0.25	60	0.75	8511	32	8100	1.33	4445
50/1/0.25	120	0.90	11638	38	9600	1.3	9812
25/1/0.25	7	0. 38	2690	21	5400	1.26	2390
25/1/0.25	15	0.56	4391	26	6500	1.34	3099
25/1/0.25	22	0.67	4517	26	6700	1.27	3361
25/1/0.25	30	0.75	5006	27	6800	1.28	3885
100/1/0.25	7	0.38	10252	37	9300	1,34	6627
100/1/0.25	15	0.49	12556	40	10000	1.74	8829
100/1/0.25	22	0.58	15297	44	11100	2.08	10060
100/1/0.25	30	0.78	20897	51	12800	1.69	16955
25/1/0.25	7	0.18	1964	20	5085	1.13	773
25/1/0.25	15	0.45	3069	21	5320	1.22	1367
25/1/0.25	22	0.58	4399	23	5850	1.25	4384
25/1/0.25	30	0.81	4787	27	6800	1.27	5154
25/1/0.125	7	0.35	2204	21	5370	1.1	3196
25/1/0.125	15	0.41	2899	22	5500	1.21	3363
25/1/0.125	22	0.48	3298	22	5500	1.25	3591
25/1/0.125	30	0.83	5558	28	7030	1.33	4350

APPENDIX C

RAFT POLYMERIZATION OF PEGMA

Sample Code	Mn GPC	PDI	Mn NMR	DP
DT/PEGMA/1	8000	1.14	6000	13

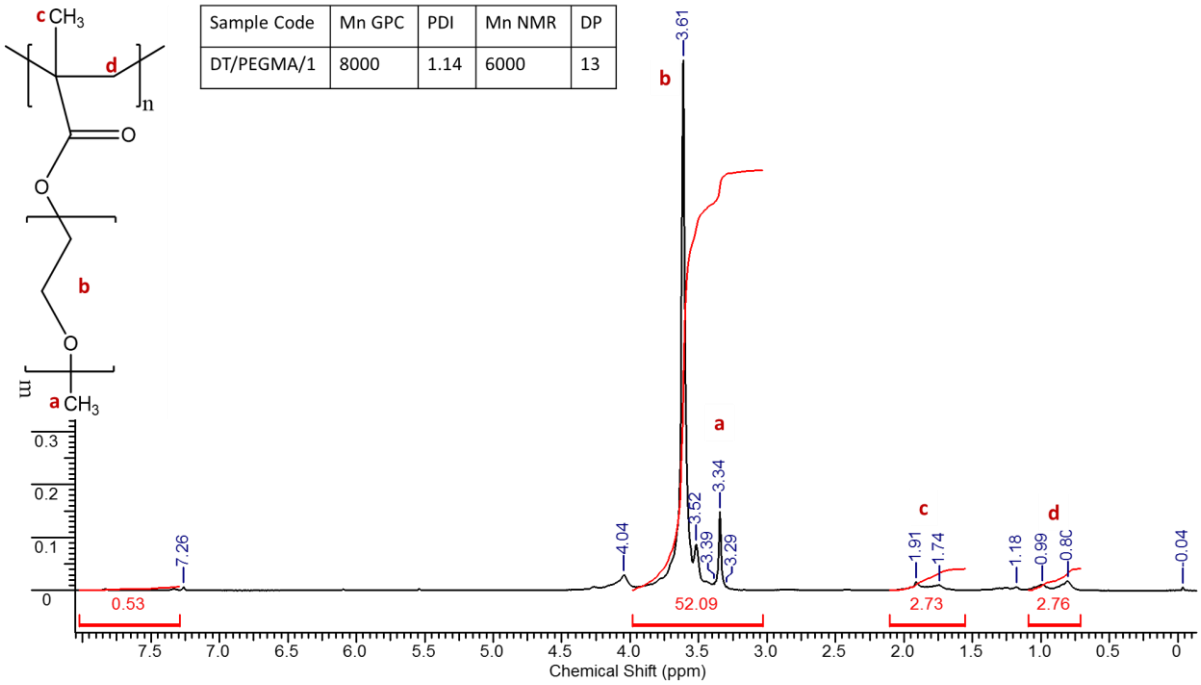

Figure C 1. ^{1}H-NMR spectrum of PPEGMA after purification. The polymer was obtained using the following polymerization conditions (Monomer Concentration: 1M and [M]/[R]/[I]: 50/1/0.25 at 65^{o}C)

APPENDIX D

MODIFICATION REACTION OF PPFMA WITH AME

Table D 1. Reaction conditions for modification of PPFMA with AME

PPFMA: AME: TEA (mol ratio)	Modification Yields (%) (obtained from ^{19}F NMR and Equation 3.3 in Chapter 3)
1/1/1	35
1/1/2	49
1/2/2	80
1/3/3	41
1/1/3	100

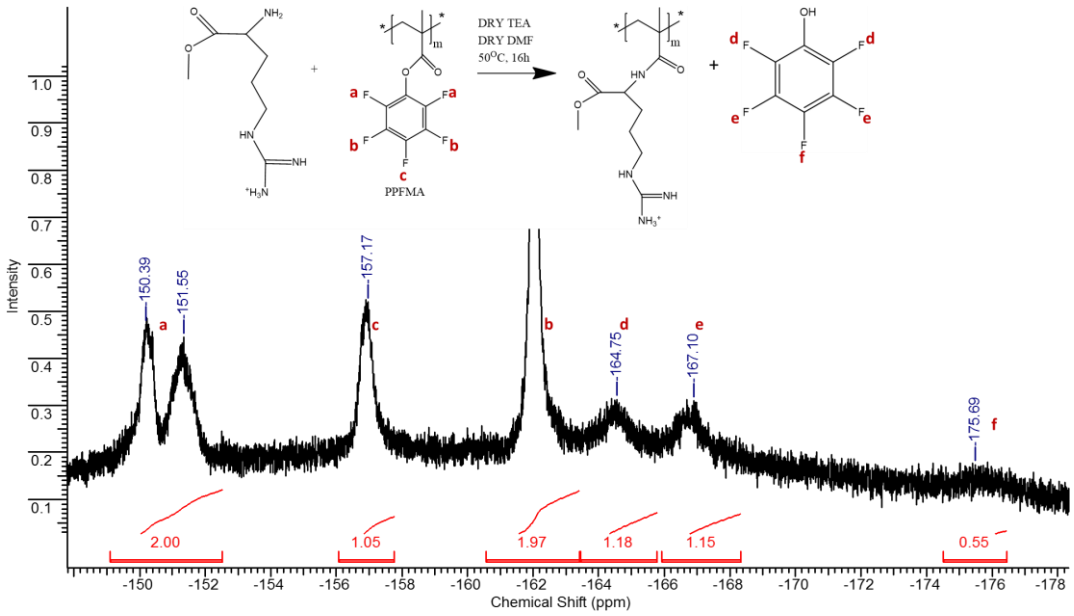

Figure D 1. ^{19}F-NMR spectrum of AMEmodified PPFMA (PPFMA/AME/TEA mol ratio: 1/2/2)